Degradation of lingual orthodontics archwires
The effect of corrosion and nickel release on their properties

Carlos Suárez Martínez

Directors

Dr. María Teresa Vilar Martínez (UB)
Dr. Francesc Xavier Gil Mur (UPC)

Department of Odontostomatology
PhD Program: Clinical Techniques in Odontostomatology (2003-2005)

Faculty of Dentistry. University of Barcelona
4th of December 2007

3. Results

3.1 OCP

Respond wires OCP ranged from -350 mV to -563,56 mV being the average value -454,81 mV.

D-Rect wires OCP ranged from 90,94 mV to -715,62 mV being the average value -310,73 mV.

Stainless Steel 0.016x0.022 OCP ranged from -92,56 mV to -403 mV being the average value -306,38 mV.

Stainless Steel 0.016 OCP ranged from -423,25 mV to -578,56 mV being the average -525,12 mV.

NiTi wires OCP ranged from 270,25 mV to -261,31 mV with an average value of 46,36 mV.

CuNiTi wires OCP ranged from 123,32 mV to -248,75 mV and an average value of -76,06 mV.

TMA wires OCP ranged from 174,25 mV to -286,81 mV and an average value of -93,02 mV.

Results are gathered in table 4. Graph 9 and 10 show the individual measurements and the average trend for the measurements respectively. Graphs 11 to 17 show the individual OCP records for the specimens tested of the alloys. Each graph has been modified in order to obtain a regular OCP measurement given that sudden changes are considered to be ‘lab noise’. So each graph shows the original and modified measurements.

	1	2	3	4	5	average (mV)
Respond	-350	-450,87	-563,56			-454,81
D-Rect	90,94	-125,87	-492,37	-715,62		-310,73
ss 0,016	-423,25	-578,56	-573,56			-525,12
ss 0,016x0,022	-92,56	-332,87	-397,12	-403		-306,38
NiTi	193,5	269	-239,62	270,25	-261,31	46,36
CuNiTi	123,32	-102,75	-248,75			-76,06
TMA	174,25	-166,5	-286,81			-93,02

Table 4

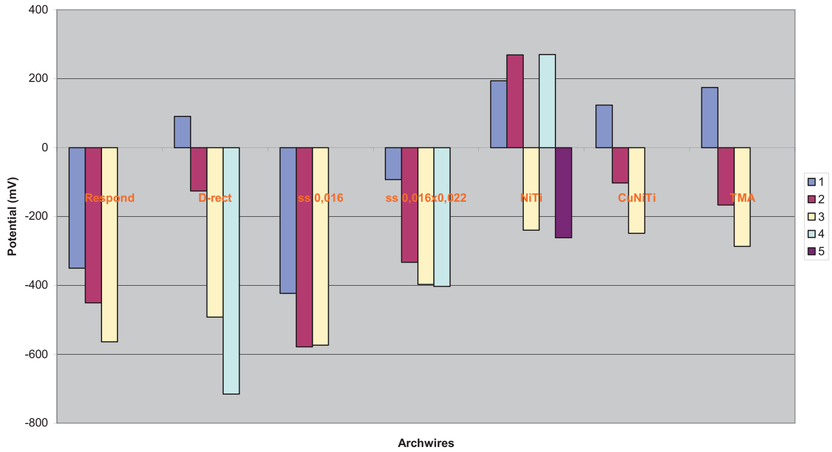

Graph 9

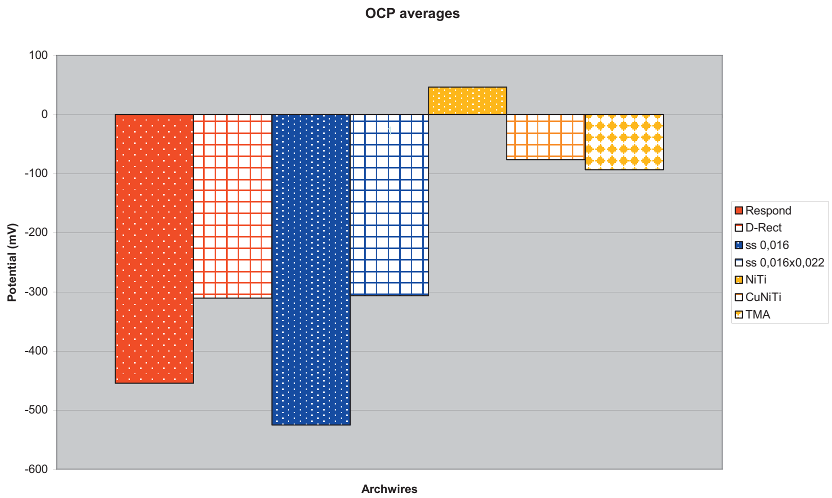

Graph 10

Graph 11


OCP Respond
0
-200
-400
-600
-800
Potential (mV)
0
20
40
60
80
100
120
140
160
180
Time (min)

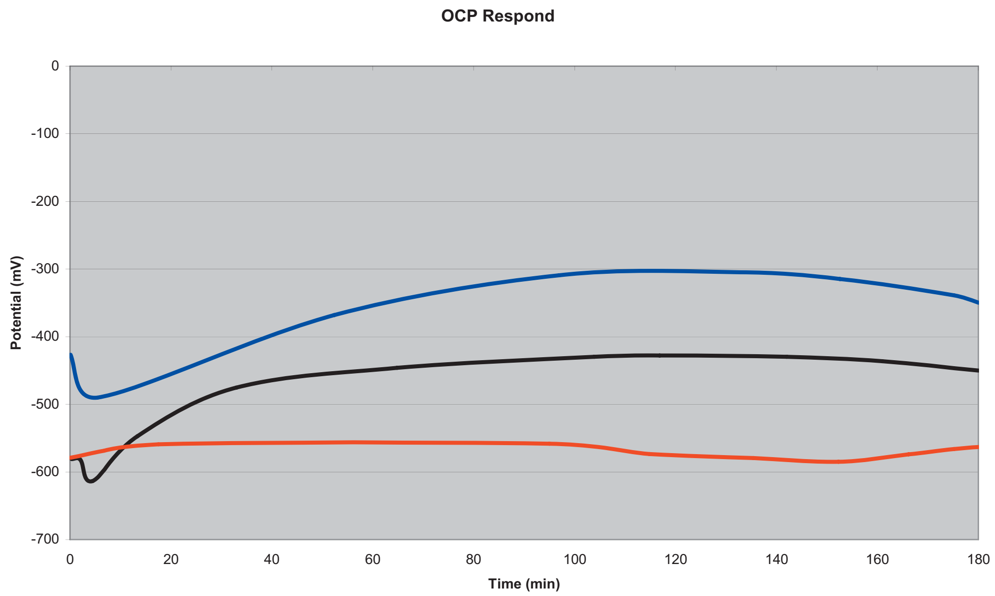
OCP Respond
0
-100
-200
-300
-400
-500
-600
-700
Potential (mV)
0
20
40
60
80
100
120
140
160
180
Time (min)

Graph 12

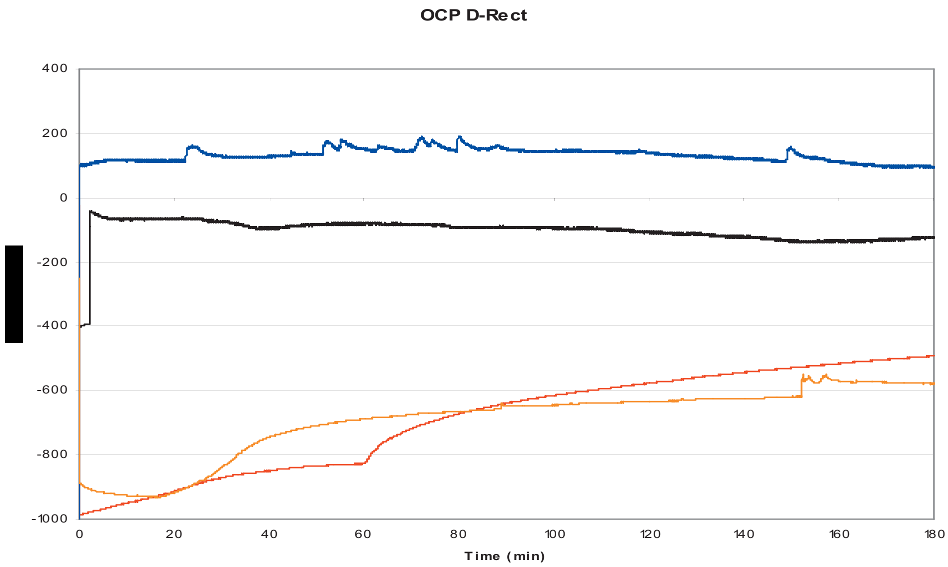
OCP D-Rect
400
200
0
-200
-400
-600
-800
-1000
[redacted]
0
20
40
60
80
100
120
140
160
180
Time (min)

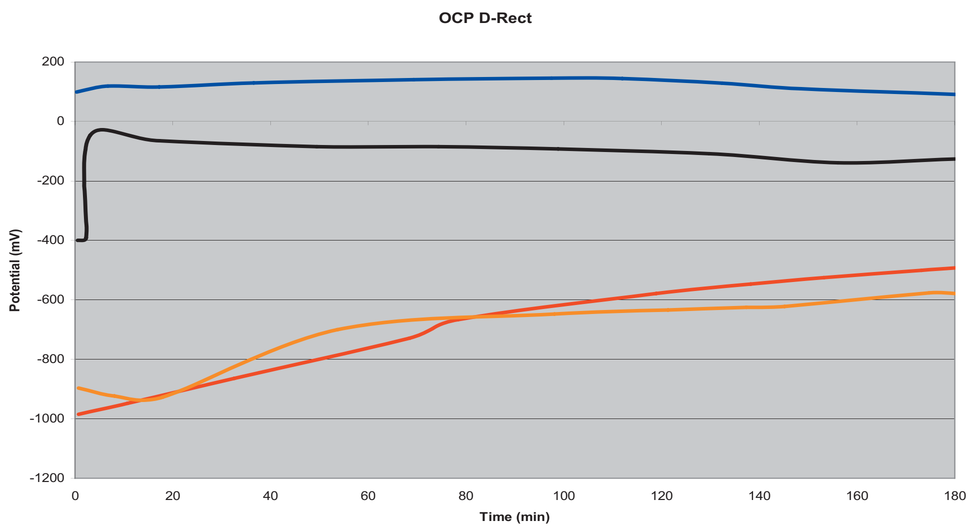
OCP D-Rect
200
0
-200
-400
-600
-800
-1000
-1200
Potential (mV)
0
20
40
60
80
100
120
140
160
180
Time (min)

Graph 13

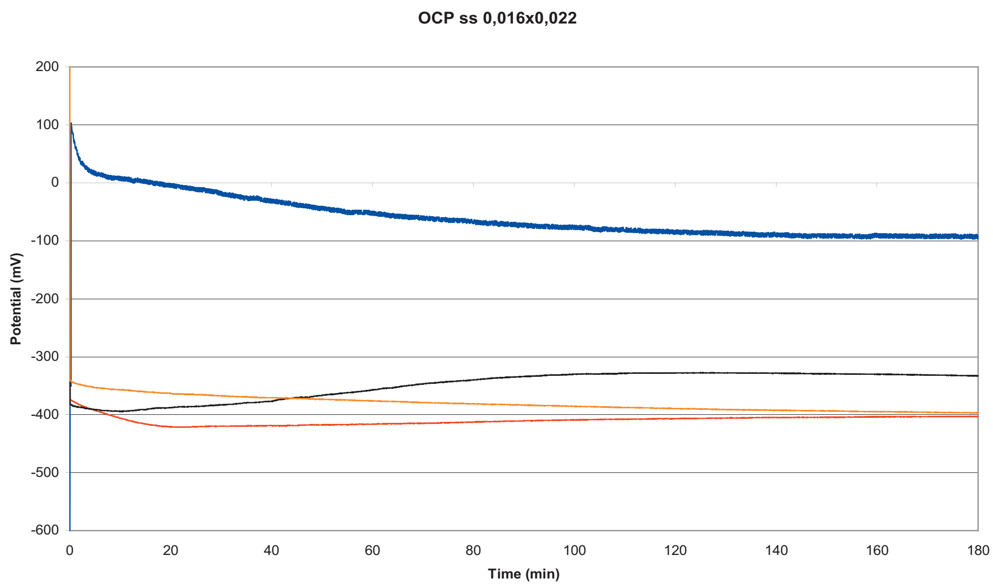
OCP ss 0,016x0,022
200
100
0
-100
-200
-300
-400
-500
-600
Potential (mV)
0
20
40
60
80
100
120
140
160
180
Time (min)

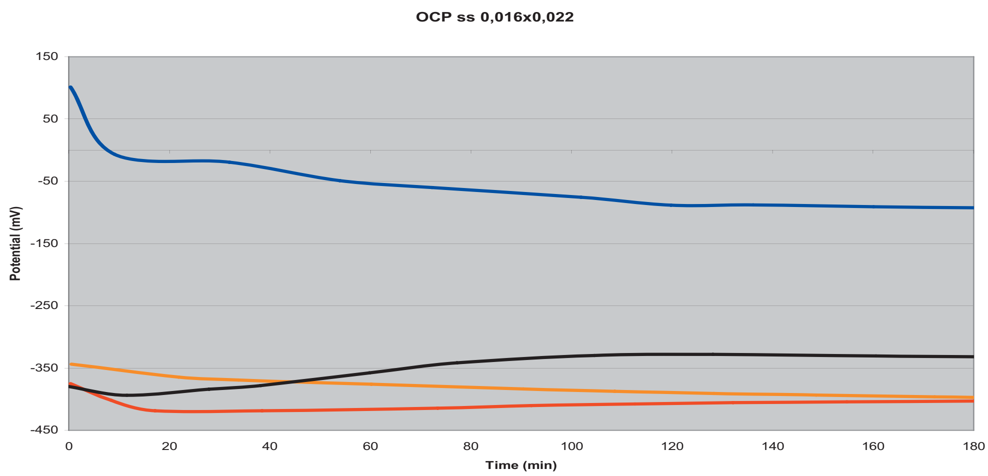
OCP ss 0,016x0,022
150
50
-50
-150
-250
-350
-450
Potential (mV)
0
20
40
60
80
100
120
140
160
180
Time (min)

Graph 14

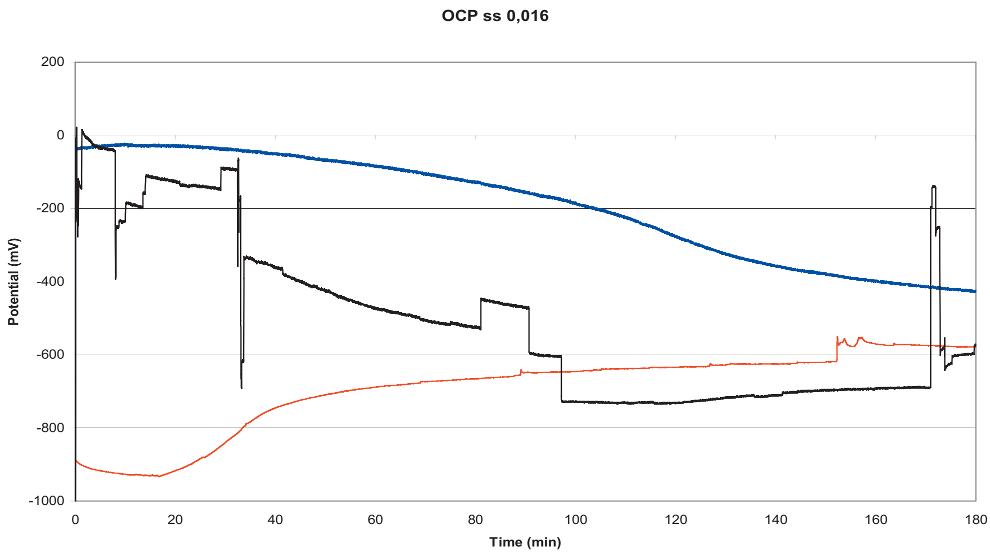
OCP ss 0,016
Potential (mV)
Time (min)
200
0
-200
-400
-600
-800
-1000
0
20
40
60
80
100
120
140
160
180

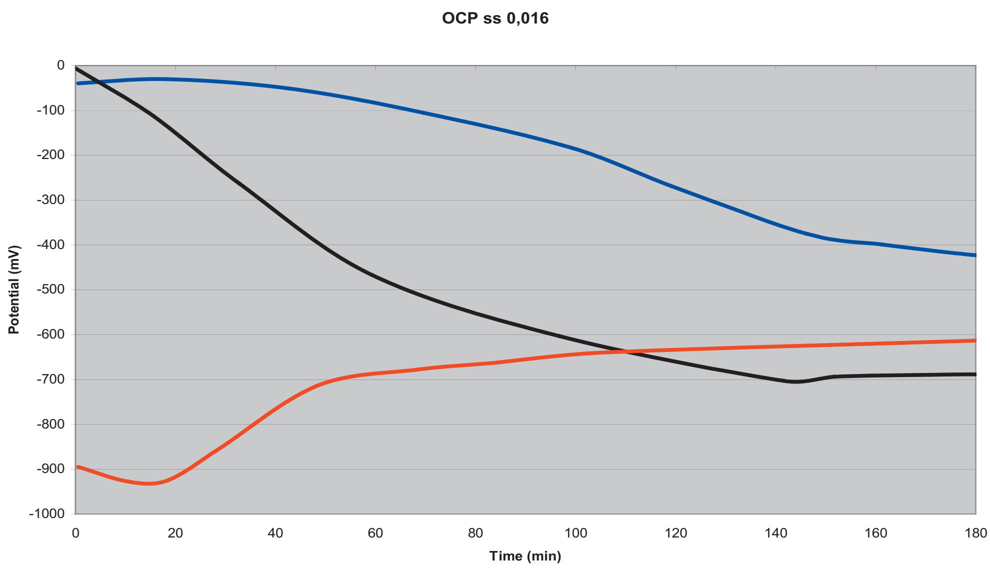
OCP ss 0,016
Potential (mV)
Time (min)
0
-100
-200
-300
-400
-500
-600
-700
-800
-900
-1000
0
20
40
60
80
100
120
140
160
180

Graph 15

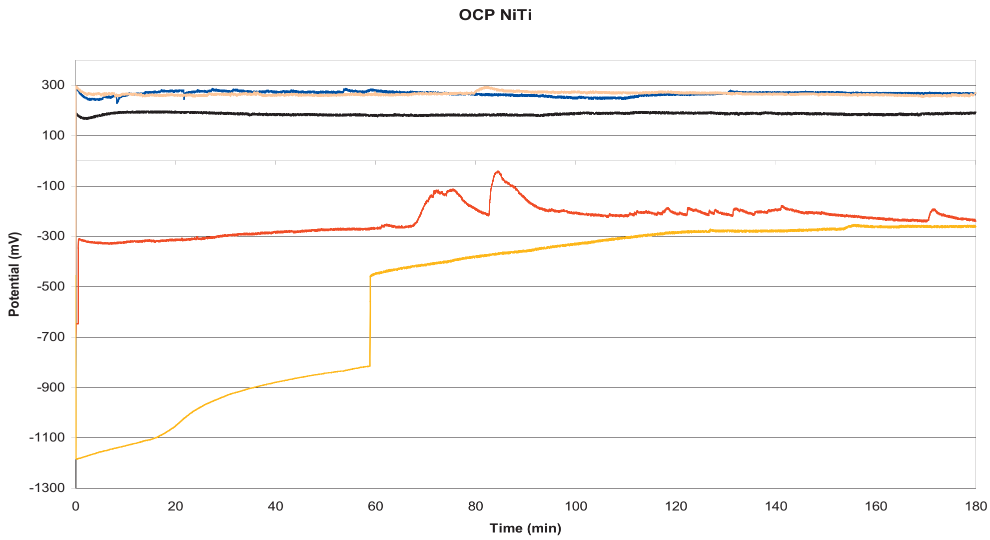

OCP NiTi
300
100
-100
-300
-500
-700
-900
-1100
-1300
Potential (mV)
0
20
40
60
80
100
120
140
160
180
Time (min)

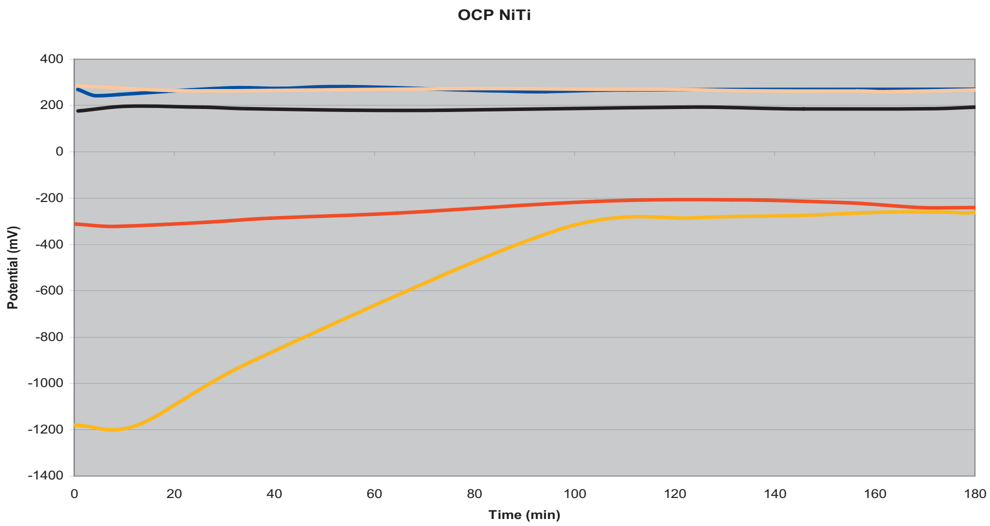

OCP NiTi
400
200
0
-200
-400
-600
-800
-1000
-1200
-1400
Potential (mV)
0
20
40
60
80
100
120
140
160
180
Time (min)

Graph 16

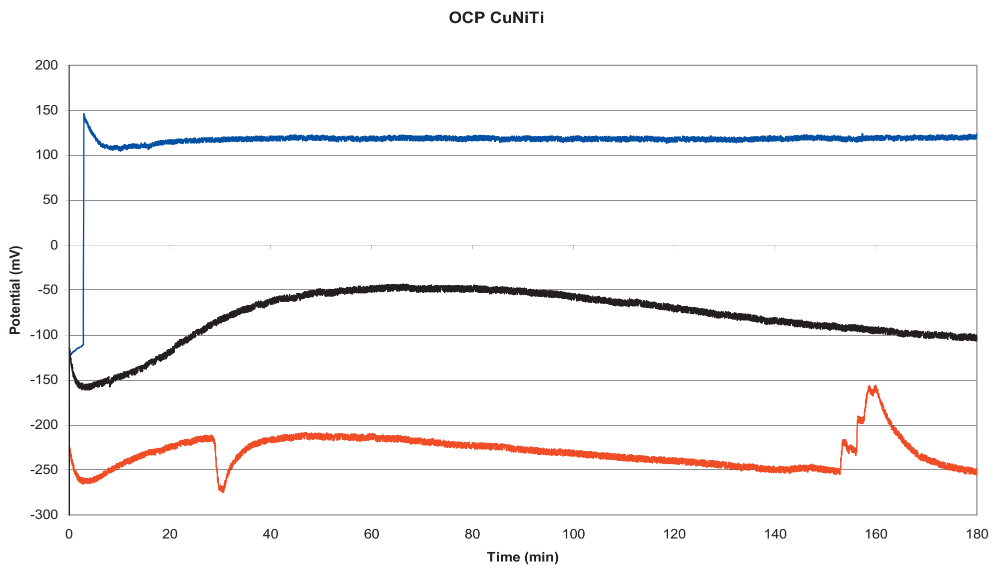
OCP CuNiTi
200
150
100
50
0
-50
-100
-150
-200
-250
-300
Potential (mV)
0
20
40
60
80
100
120
140
160
180
Time (min)

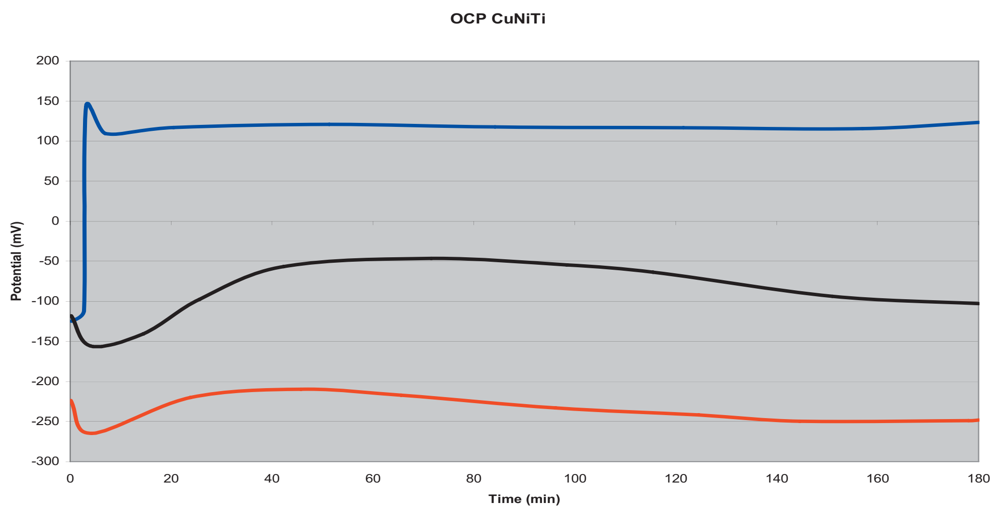
OCP CuNiTi
200
150
100
50
0
-50
-100
-150
-200
-250
-300
Potential (mV)
0
20
40
60
80
100
120
140
160
180
Time (min)

Graph 17

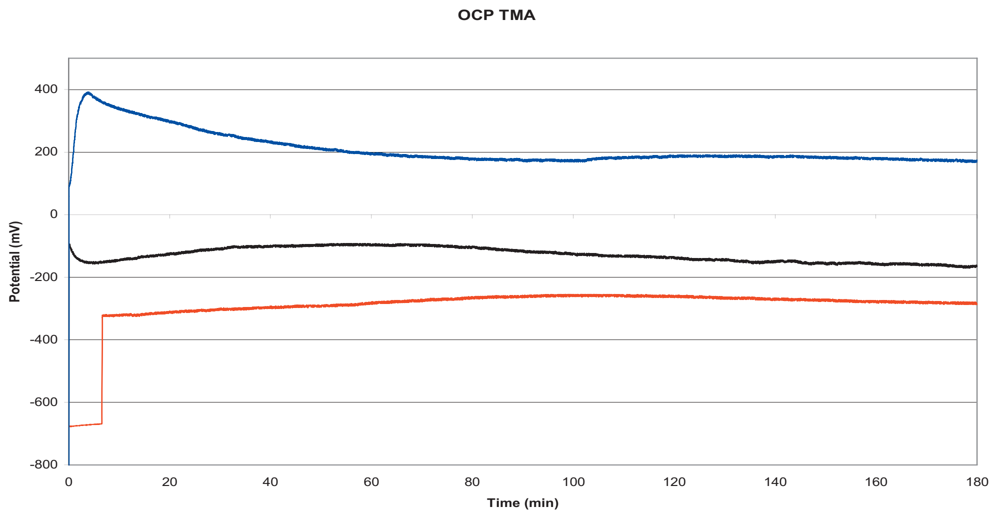

OCP TMA
Potential (mV)
400
200
0
-200
-400
-600
-800
0
20
40
60
80
100
120
140
160
180
Time (min)

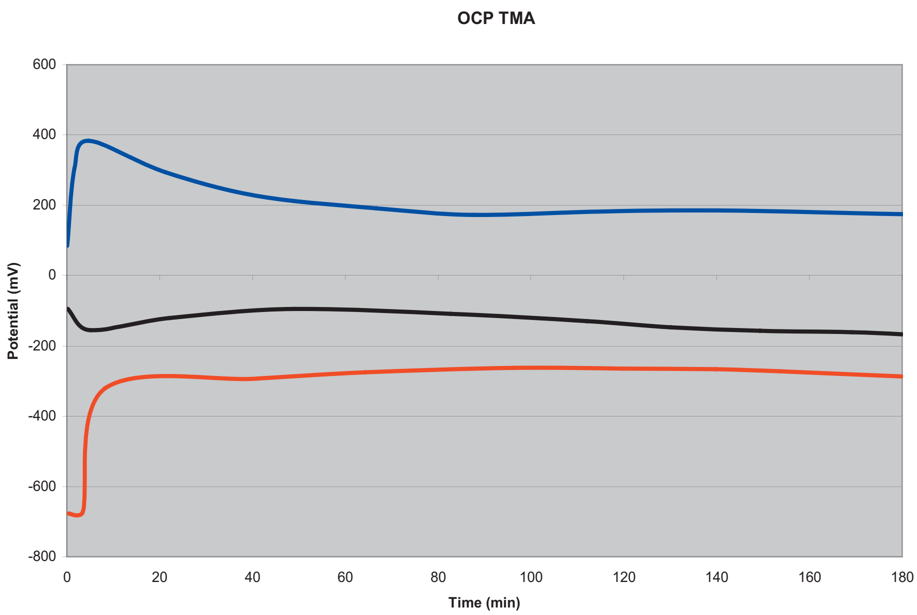

OCP TMA
Potential (mV)
600
400
200
0
-200
-400
-600
-800
0
20
40
60
80
100
120
140
160
180
Time (min)

The wires could be classified into three groups according to the OCP behavior:

1. The braided wires (Respond and D-Rect) and the 0.016 stainless steel showed similar results.

2. The 0.016x0.022 stainless steel's group showed slightly different results than the rest of the stainless steel wires.

3. The Titanium alloys whose results were are also very similar to each other.

3.2 Cyclic Voltammetry

Cyclic Voltammetry results are shown in graphs 18-24 resulting from the data gathered in the voltalab. Two graphs are shown for each alloy. First a general graph that shows the whole picture of the cyclic voltammetry test and a second graph that is a zoomed view of the points where a current flow starts to be detected and recorded by the computer.

Graph 18

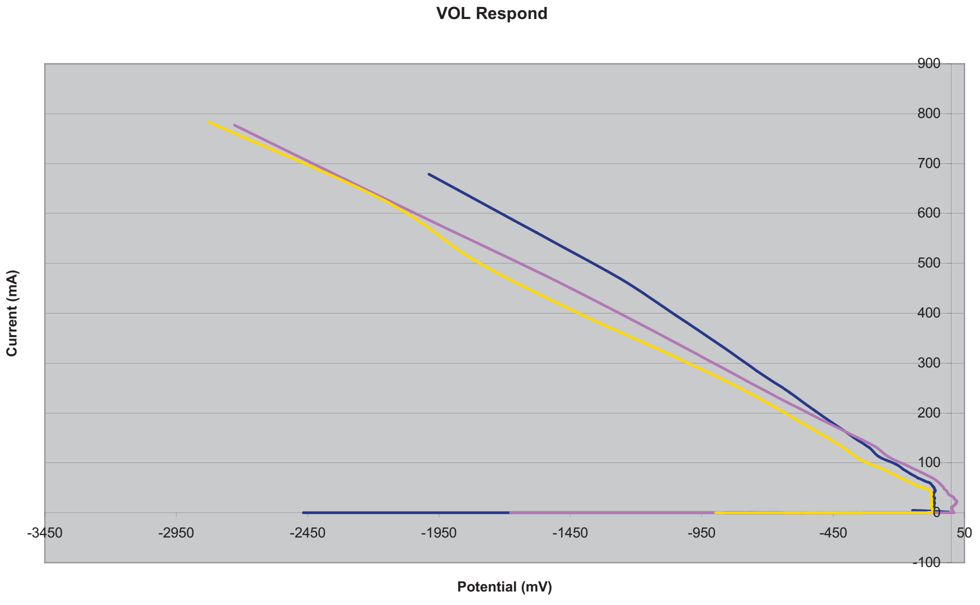

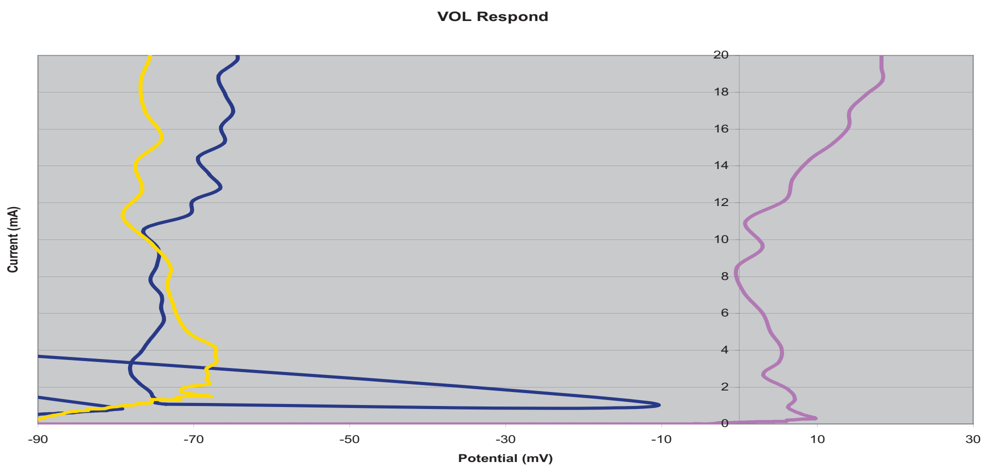

Specimens code: 1, 3, 4

Graph 19

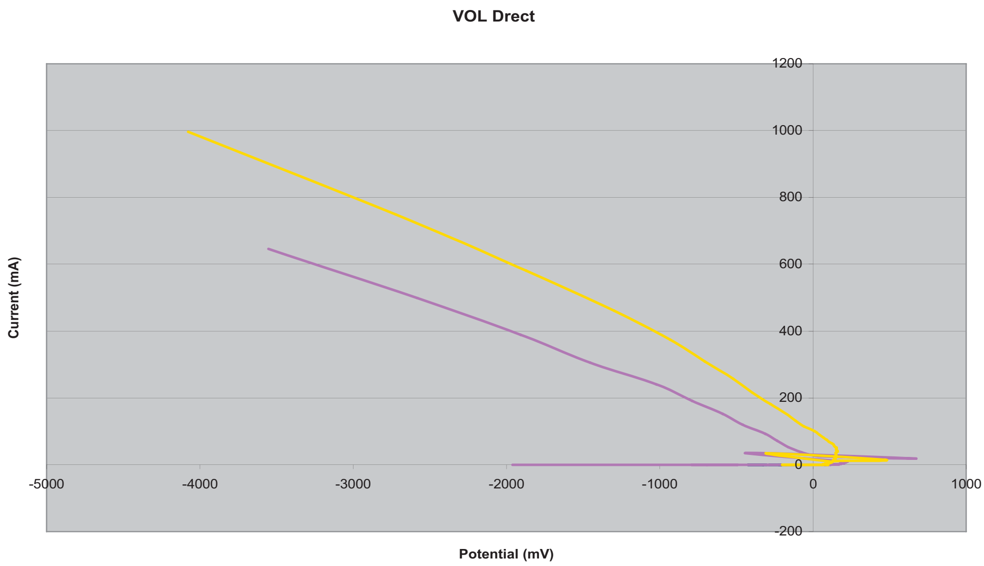

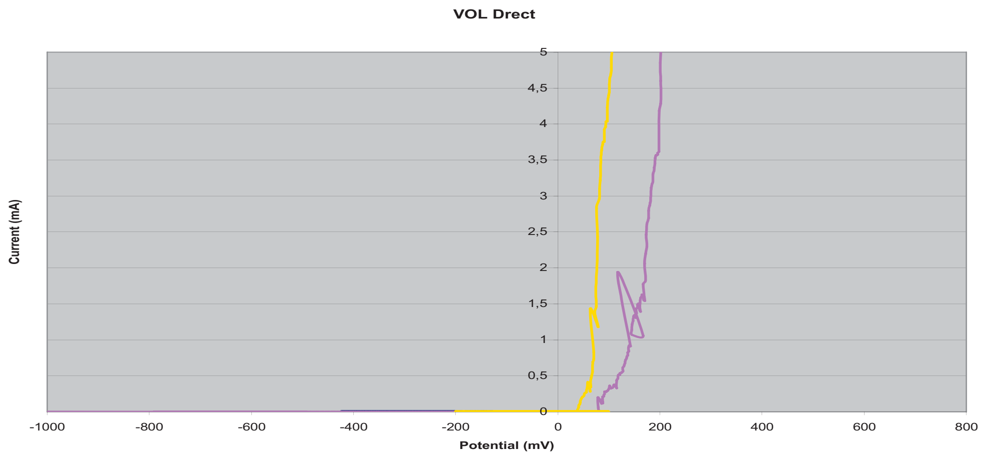

Specimens code: 1, 2, last

Graph 20

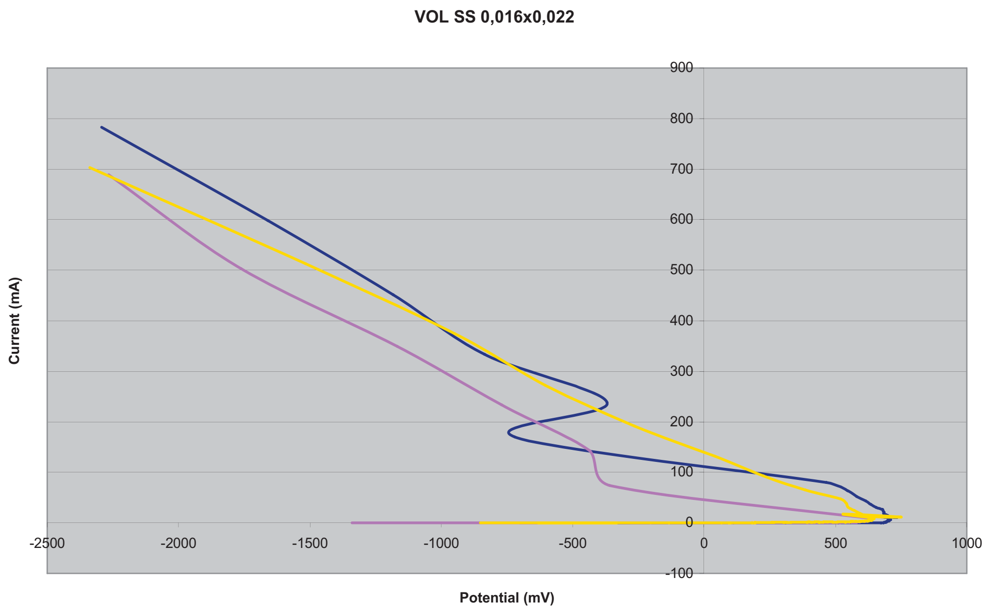

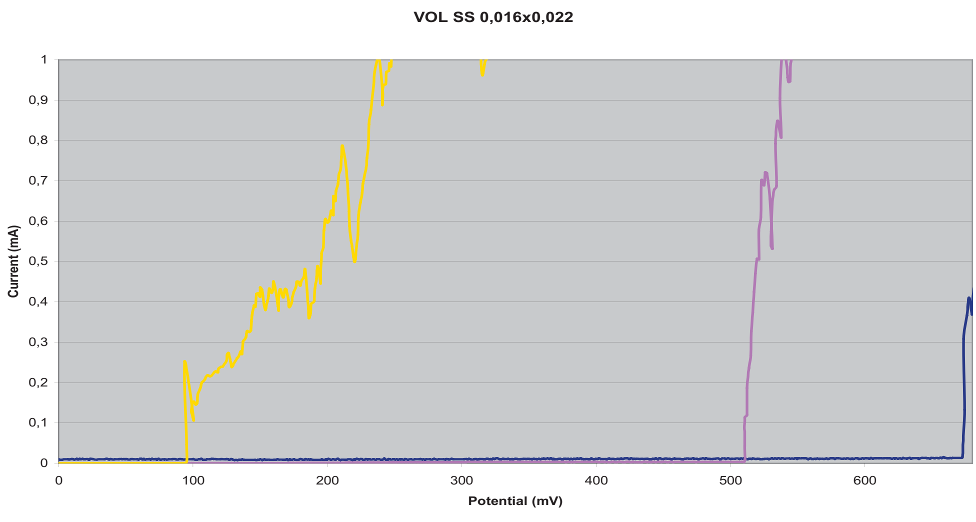

Specimen code: 1, 3, 4

Graph 21

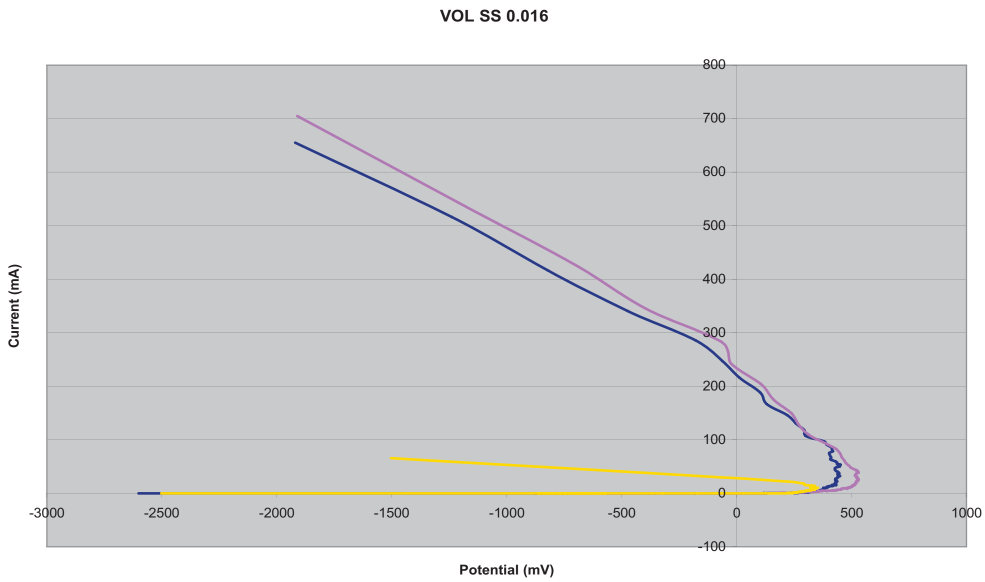

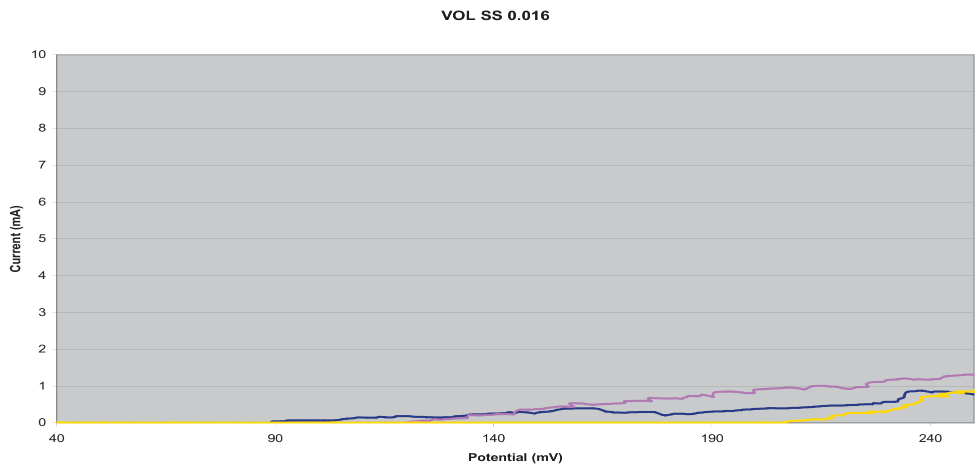

Specimen code: last, 1, 2

Graph 22

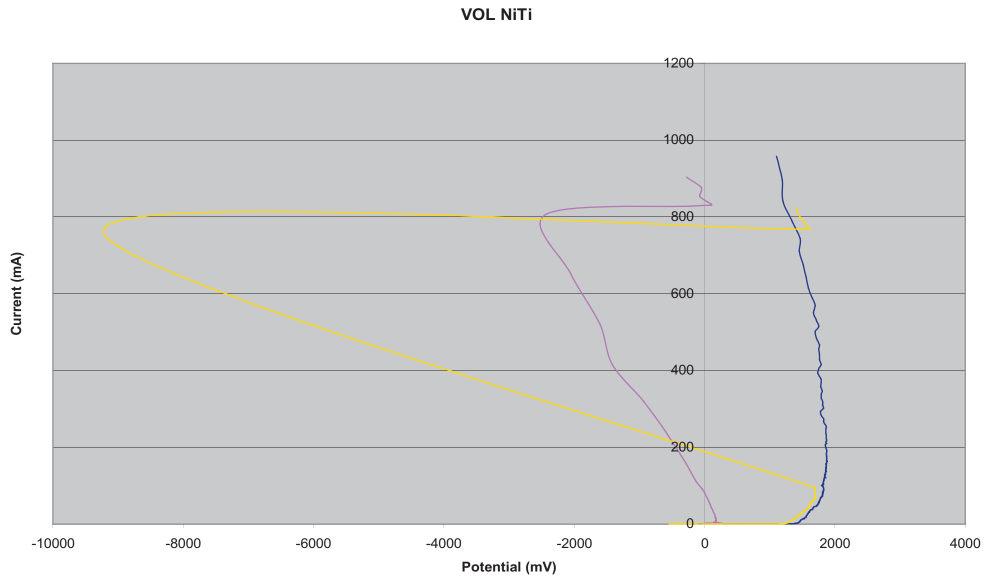

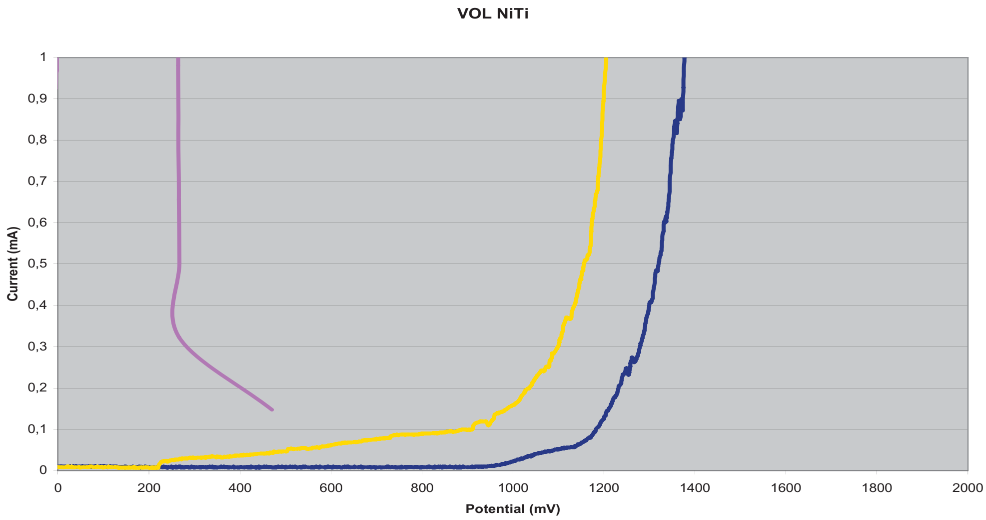

Specimens code: 4, 3, 7

Graph 23

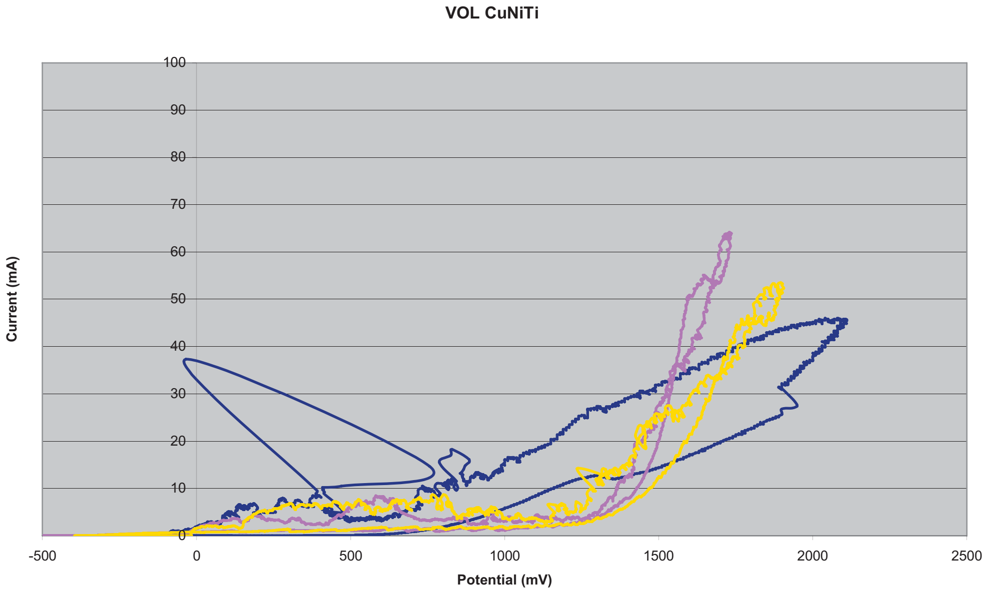

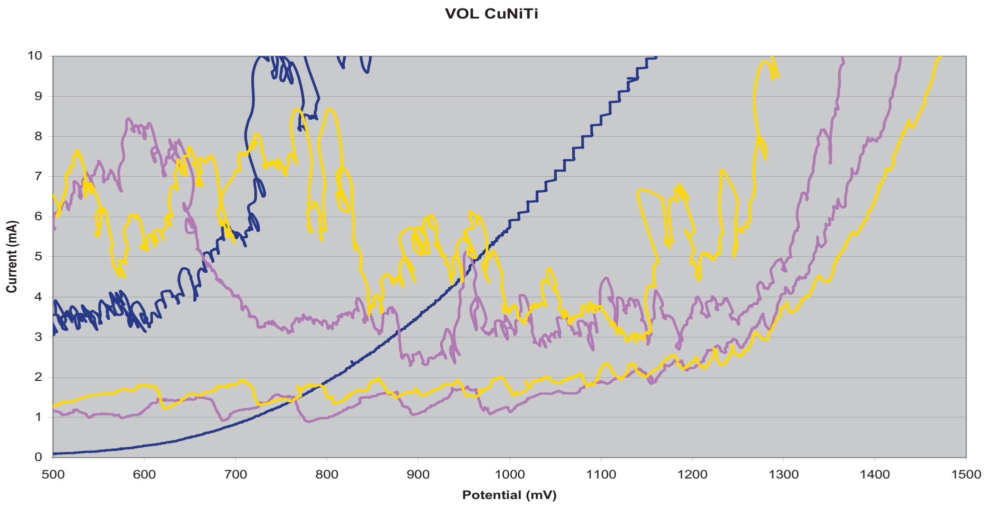

Specimens code: 1, 8, 10

Graph 24

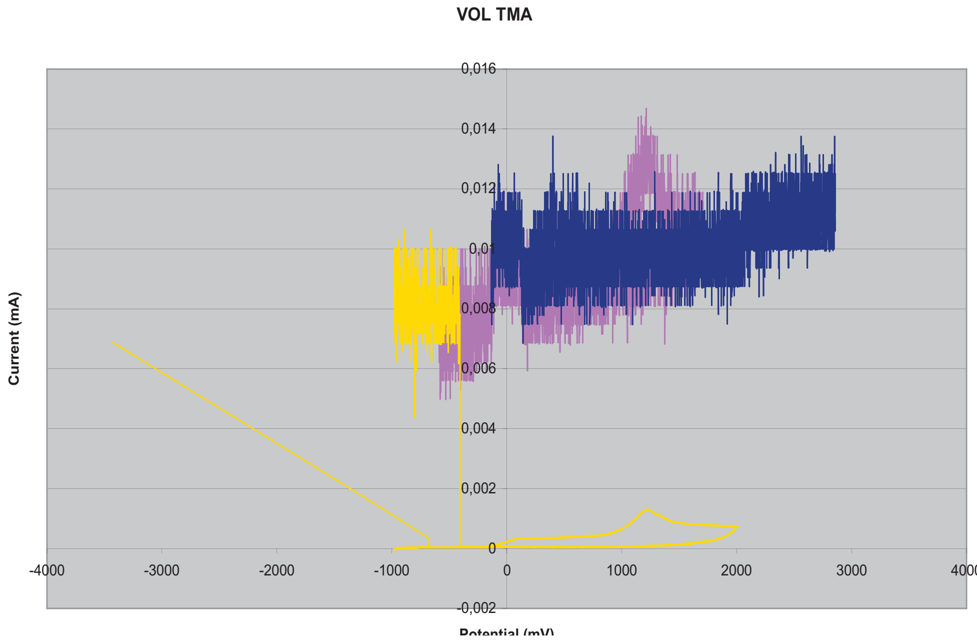

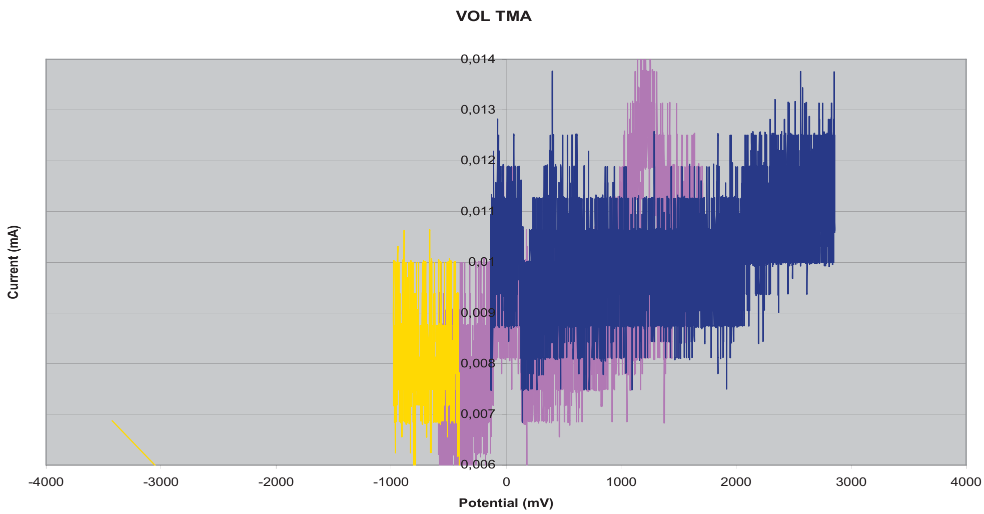

Specimen code: 2, 4, 5

According to the tested wires the potential values at which current flow started to be detected are as follows:

Respond (see graph 18)

Specimen	Potential
1	-75 mV
3	10 mV
4	-70 mV

D-Rect (see graph 19)

Specimen	Potential
Last	41 mV
2	79 mV

Stainless Steel 0.016x0.022 (see graph 20)

Specimen	Potential
1	673 mV
3	510 mV
4	95 mV

Stainless Steel 0.016 (see graph 21)

Specimen	Potential
Last	90 mV
1	120 mV
2	205 mV

Nickel Titanium (see graph 22)

Specimen	Potential
3	267 mV
4	1187 mV
7	950 mV

Copper Nickel Titanium (see graph 23)

Specimen	Potential
1	600 mV
8	1187 mV
10	1140 mV

Titanium Molybdenum Alloy (not meaningful, see graph 24)

These values have been obtained from the graphs using as criteria the point at which a significant change in current flow is produced according to the curve. As it can be seen from the graph the high precision of the potentiostat leads to irregular curves that have sudden changes in current flow when potential is varied. That is why a general graph is showed so this can be seen.

3.3 Photography

All archwires showed the effect of polarization when observed under magnified photographic techniques. Photos 25 to 31 show first the as-received specimen and the polarized archwire below it.

Photo 25

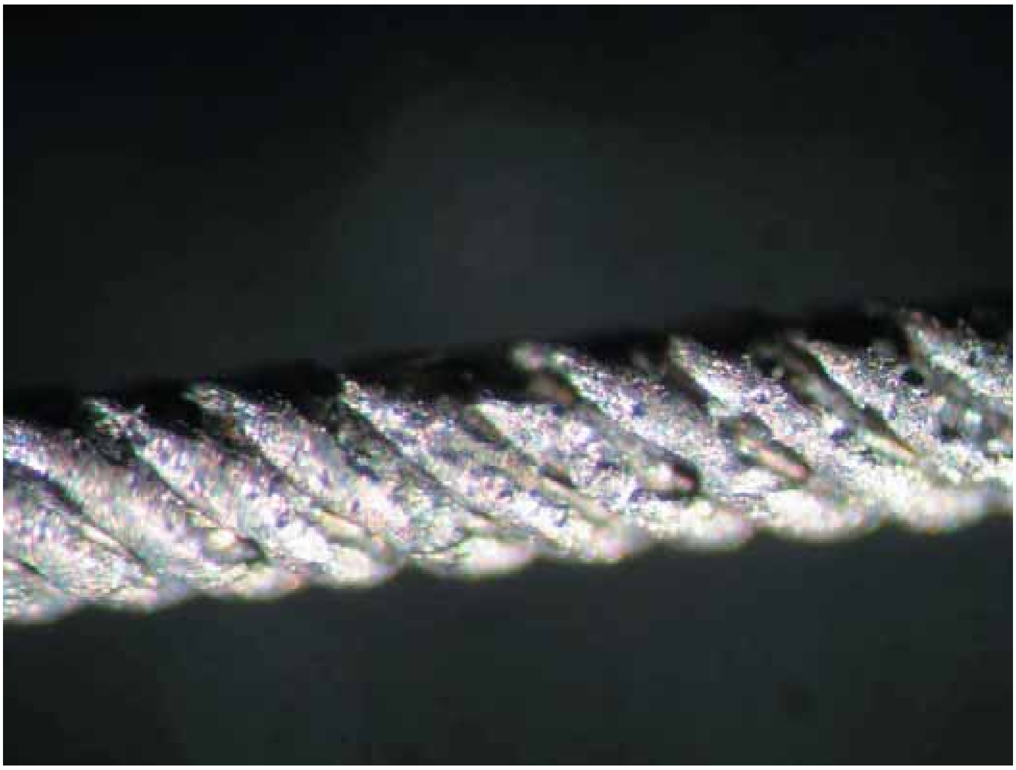

Photo 26

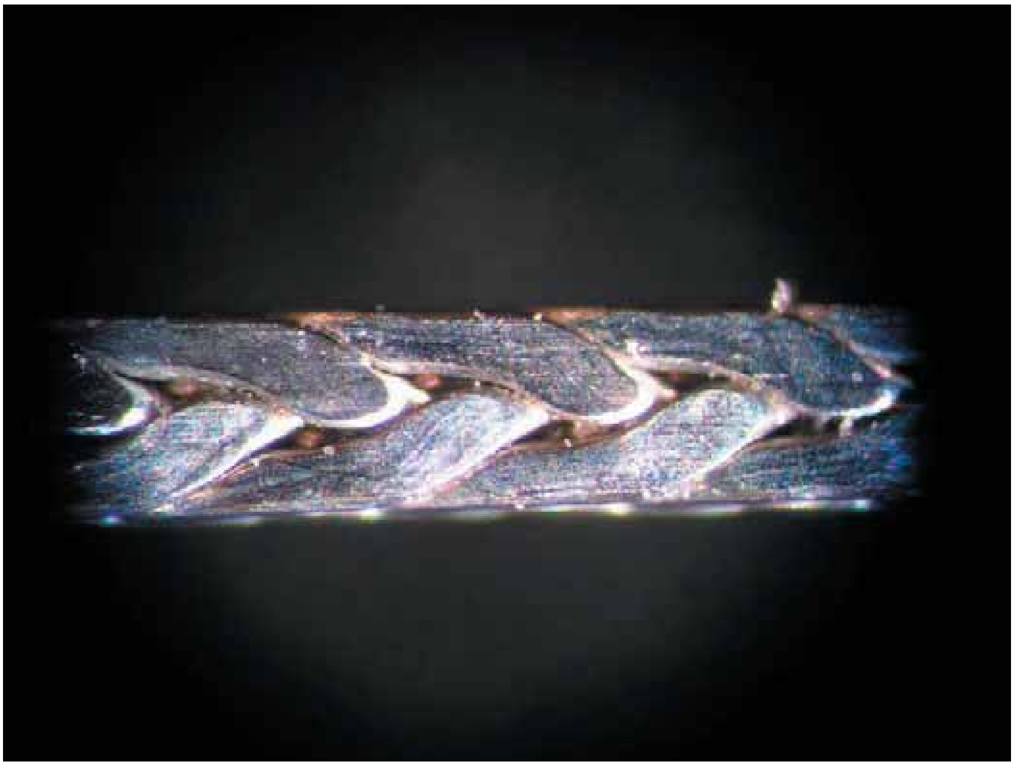

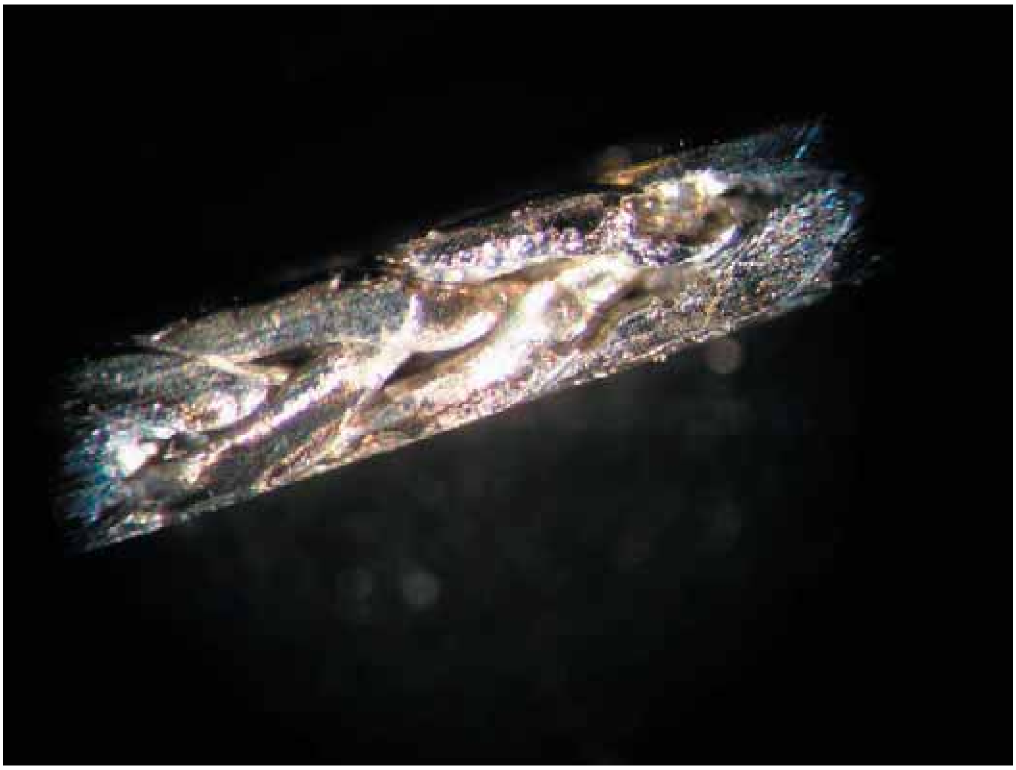

Photo 27

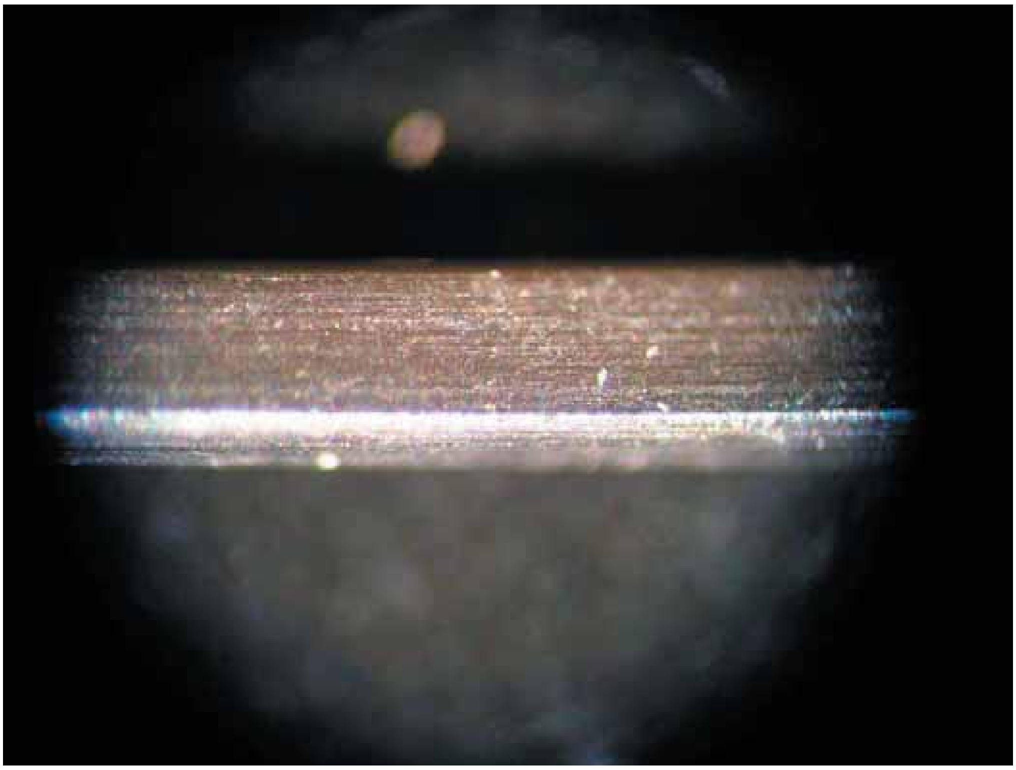

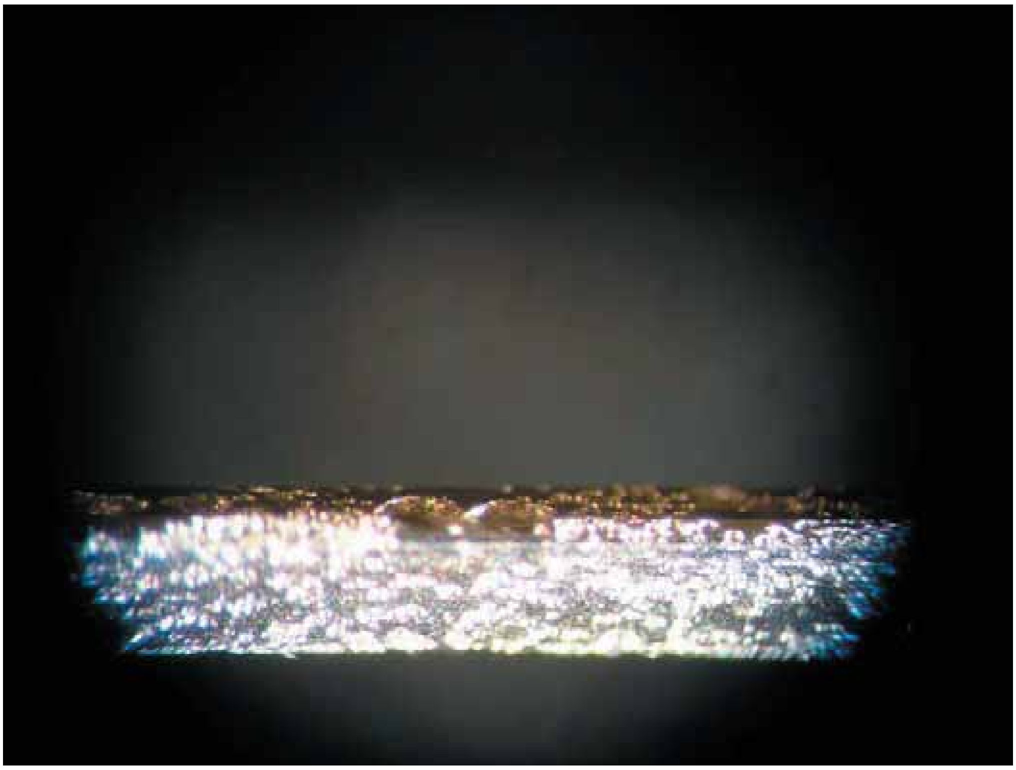

Photo 28

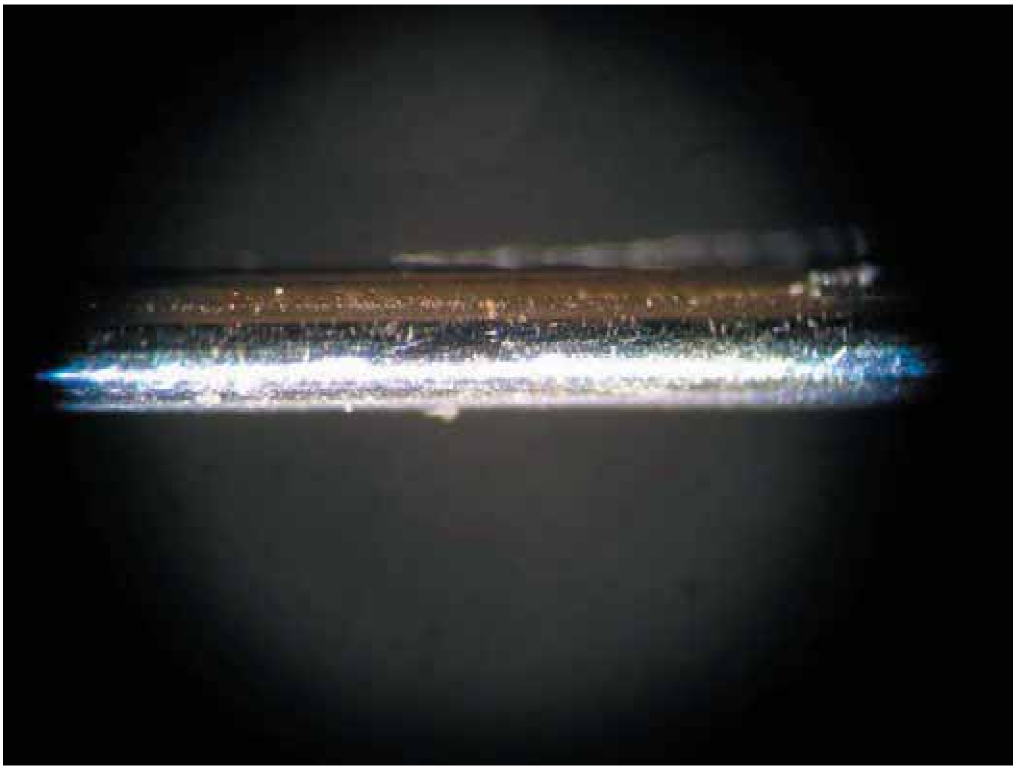

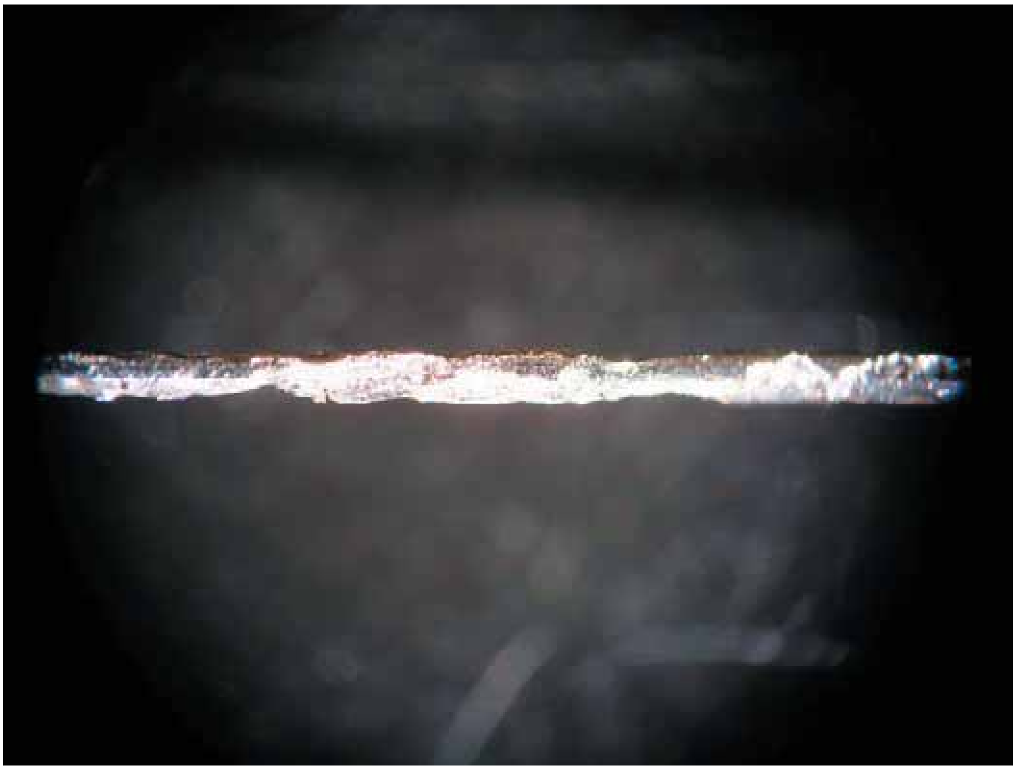

Photo 29

Photo 30

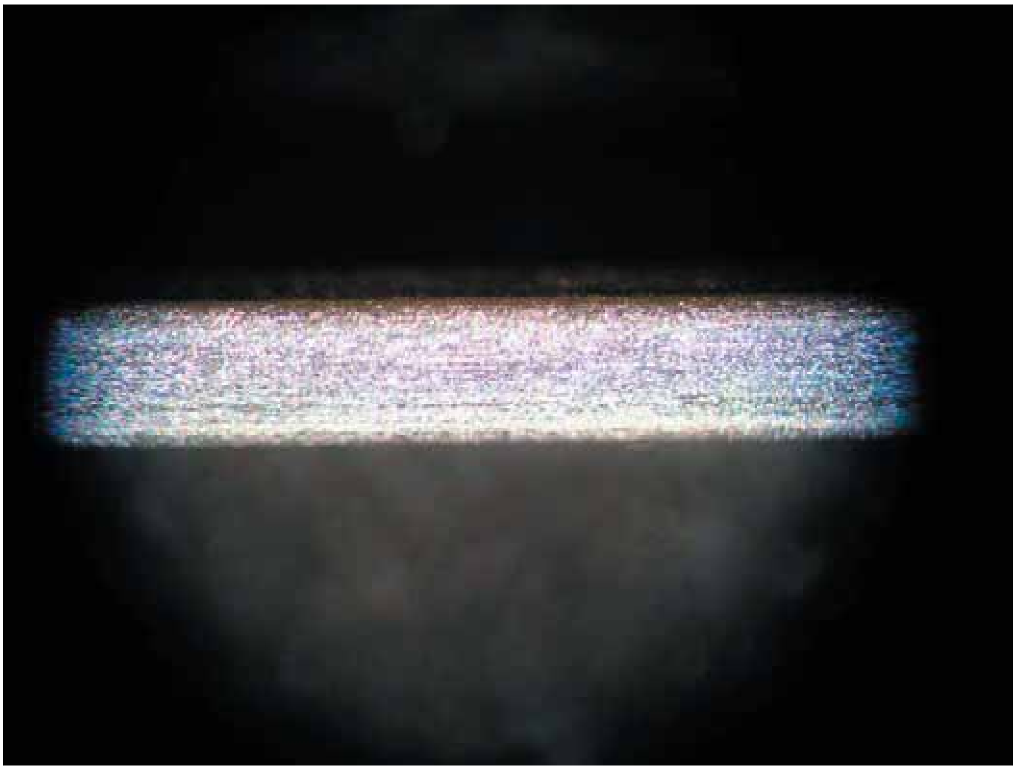

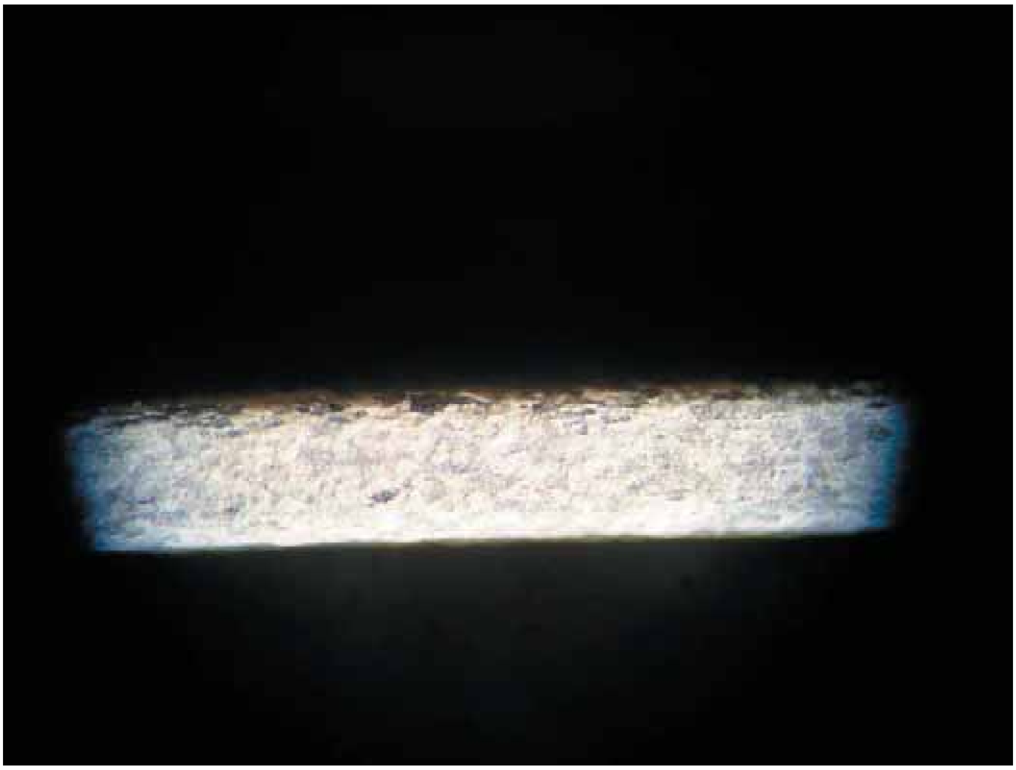

Photo 31

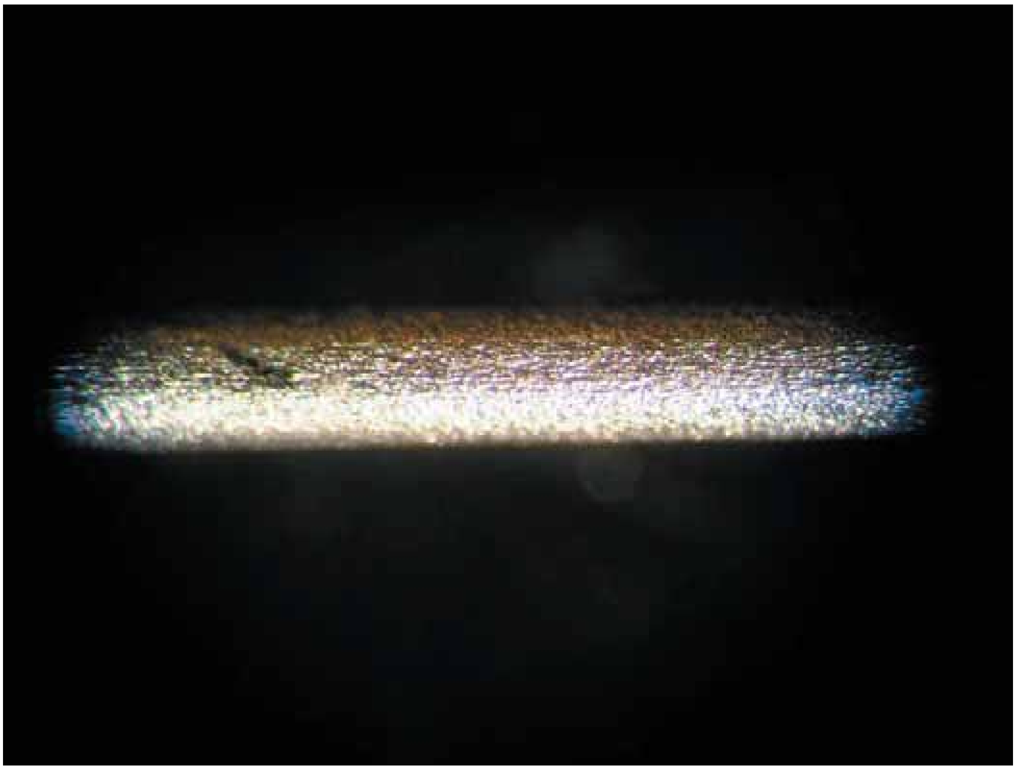

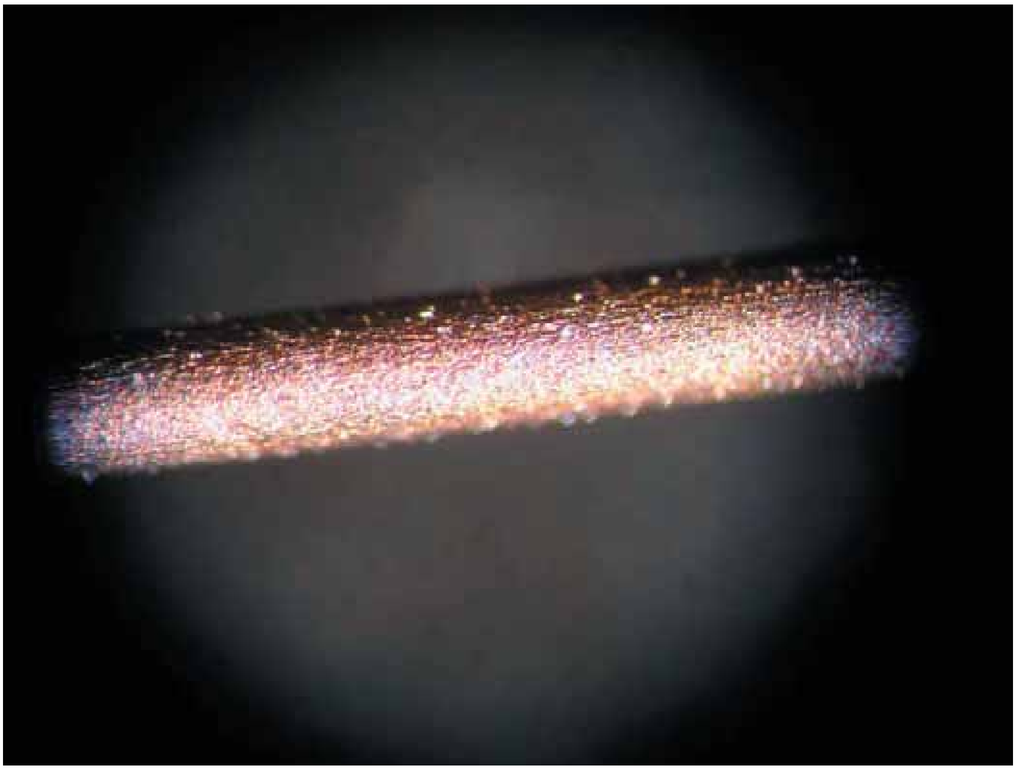

The Respond archwire (photo 25) showed a decreased shininess after polarization and an increased surface roughness as it can be seen from the photograph. Pitting corrosion can be seen all along the braided wires. A big island-like material loss that follows a particular pattern along one of the wires that form the Respond wire can also be observed. It is seen at the distal side of one of the braided wires where it contacts with the other one. It seems that the contact area is the most affected as seen from a macroscopic point of view.

D-Rect (photo 26) does not seem to have lost its shining aspect after polarization. Pitting corrosion can be observed at flat surfaces and material loss in a severe way can be also seen. This loss is an impact-like shape with rounded edges. It seems that the most affected point coincides with the archwire edge of this rectangular braided wire.

The Stainless Steel 0.016x0.022 wire (photo 27) did not lose much of its shining aspect after polarization but it did experience a massive pitting. The loss of material in an indented manner at the edge of the rectangular wire that recalls a bite was also seen in other specimens that were studied under this image technique.

The Stainless Steel 0.016 round wires (photo 28) seemed to be the most affected by polarization. The initial round section transformed into a very irregular section with a severe loss of material. Although pitting can be observed, the most spread loss of material can not be described as following a particular pattern.

NiTi round wires (photo 29) conserved their general shape quite well after polarization. From the macroscopic point of view, there is a loss of shininess of the arch that becomes very grey and rough with a surface that recalls dry paint. The surface does not seem to be affected by pitting corrosion although it can be seen that a porous like loss of surface material has occurred.

CuNiTi rectangular wires (photo 30) showed a very similar surface change after polarization. It could be compared to the NiTi change in the sense that there is a clear loss of surface shininess and the surface becomes grey. But there is a difference in the macroscopic pattern by which the loss of material is observed. In the case of these wires it is not a porous-like loss but it rather seems to be a patch-like loss in straight geometrical shapes, not rounded like NiTi wires. The edges of the wire do not seem to be particularly more affected by polarization than the rest of the area of the wire.

TMA wires (photo 31) seemed to be very resistant from the macroscopic point of view. The change in superficial shininess is difficult to assess due to the fact that polarization is followed by a change in colour from a grey colour to a red tonality. There can be seen a discrete pitting but it is not as severe as the observed in the stainless steel wires.

The effects of polarization above mentioned can be seen directly on the wires without the help of a macroscopic photographic aid. When these wires were assessed by the touch of the hands, a difference could be noticed.

Therefore, corrosive changes due to polarization can be directly observed and detected on the specimens. This should be remembered when studying them under SEM and AFM techniques that are only used in order to try to describe in a better way the surface changes that have already being found and in order to explain corrosive patterns. So corrosion is not a SEM or AFM finding, it is first of all a macroscopic finding.

3.4 Scanning Electronic Microscope

The scans taken from the SEM are presented so that the as-received state, the 30 day immersed specimen and the polarized specimen can be compared for all the archwires. Zoomed in and zoomed out images will be shown at the discussion when needed and they will be shown at different augments.

For result purposes and in order to appreciate differences the images shown at this chapter will be the x 1500 magnified of the three categories above mentioned. Each page shows the three images in the same order: as-received, 30 day immersed and polarized specimen. Representative SEM images are exposed from photo 32 to 51.

Scanning electron microscopy was also used to characterize the effects of immersion and polarization on the wire topography. Corrosive changes in surface topography were observed for all wires.

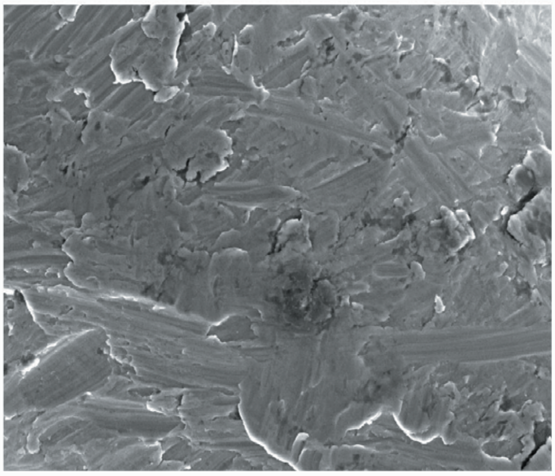

Photo 32

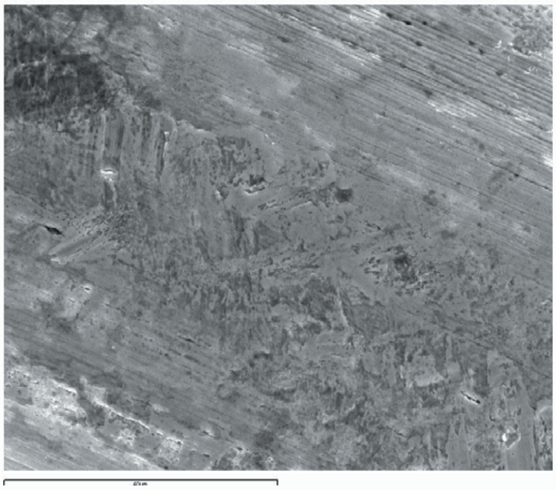

Photo 33

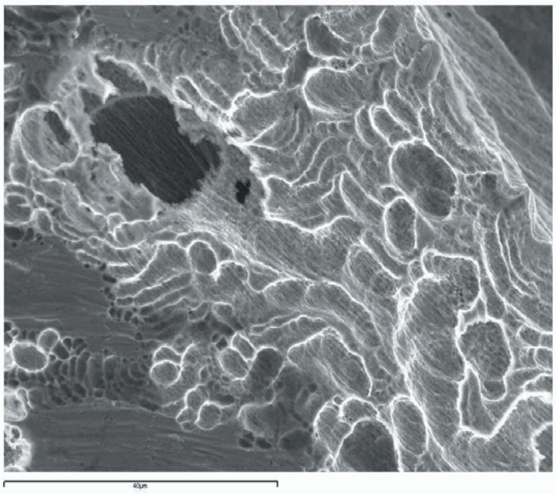

Photo 34

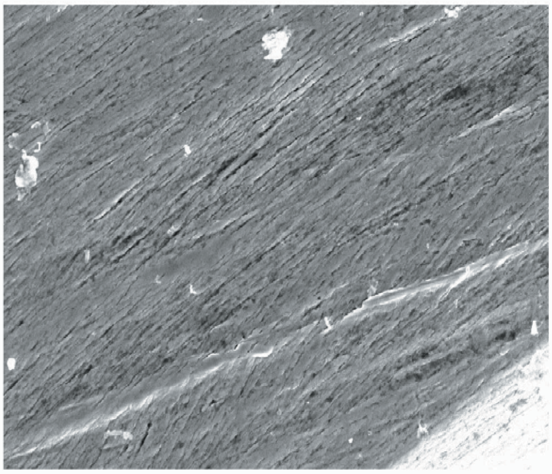

Photo 35

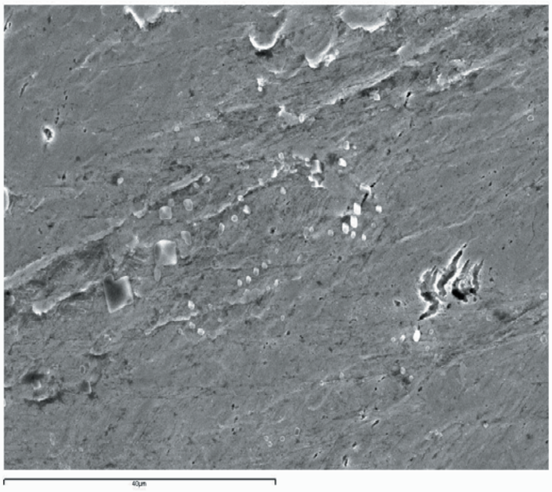

Photo 36

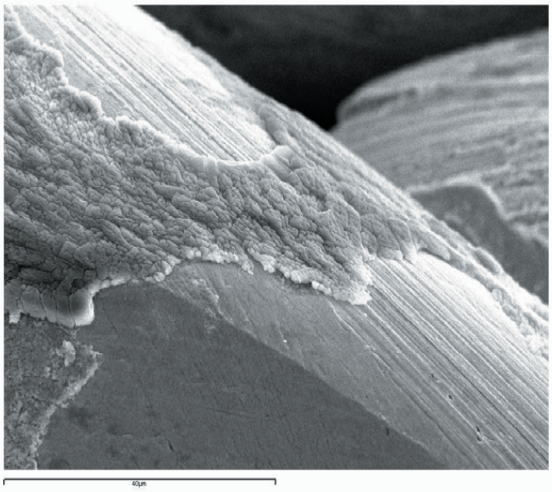

Photo 37

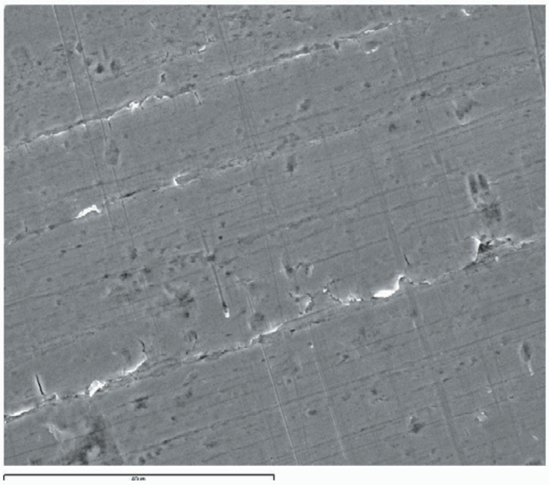

Photo 38

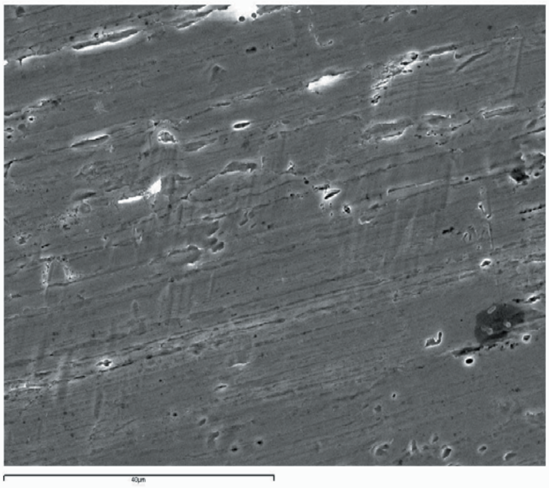

Photo 39

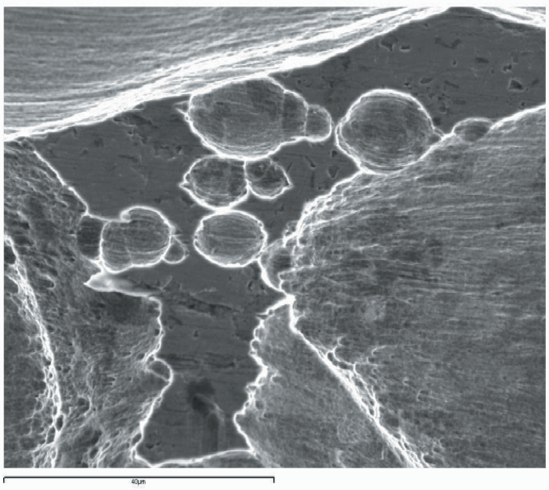

Photo 34

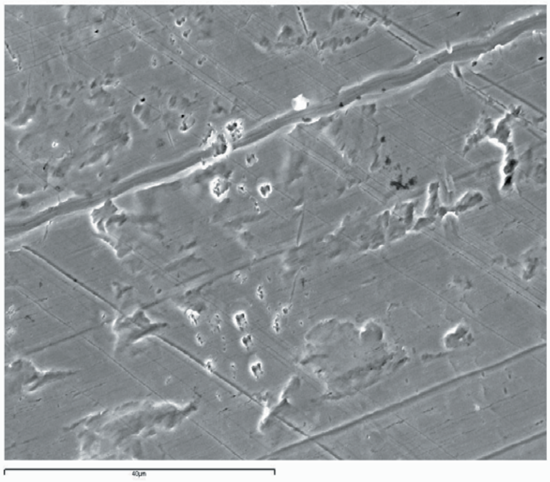

Photo 41

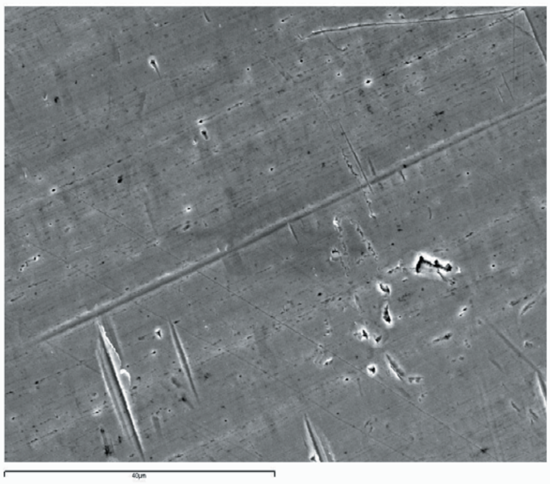

Photo 42

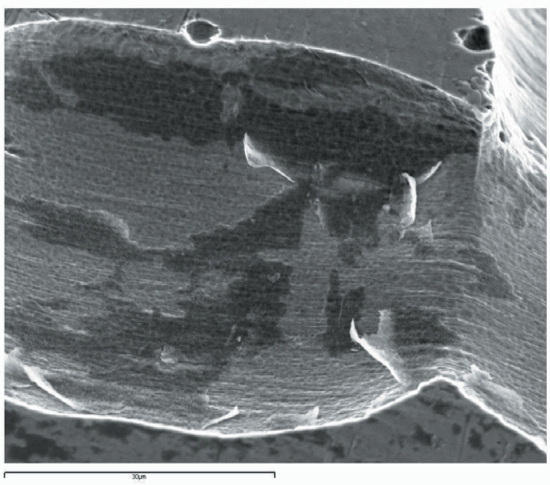

Photo 43

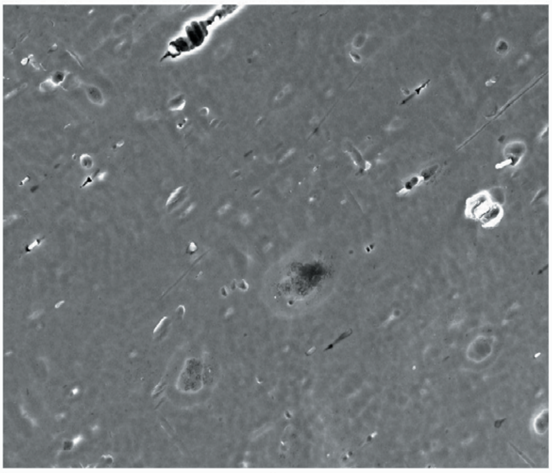

Photo 44

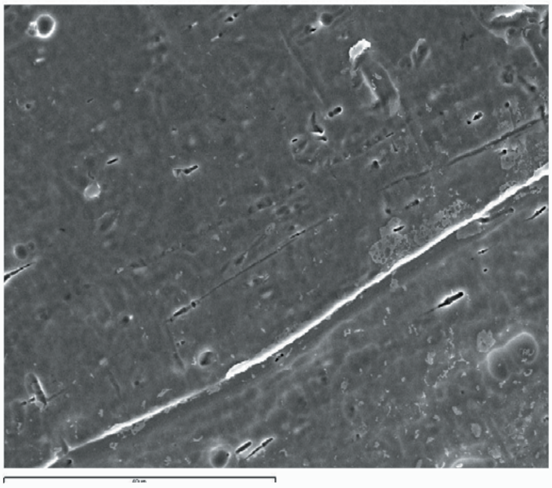

Photo 45

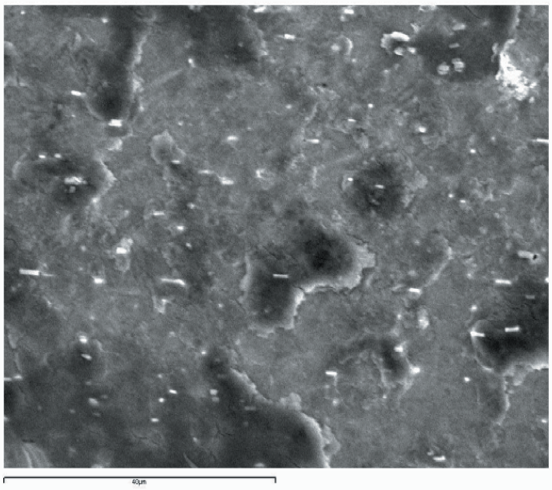

Photo 46

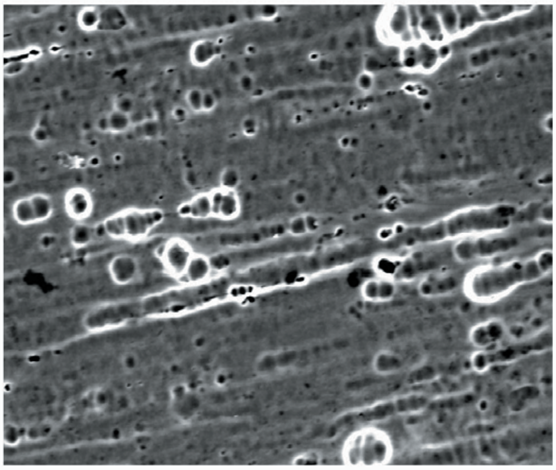

Photo 47

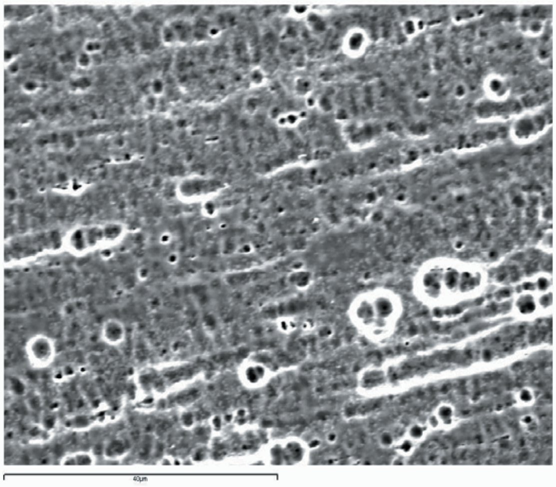

Photo 48

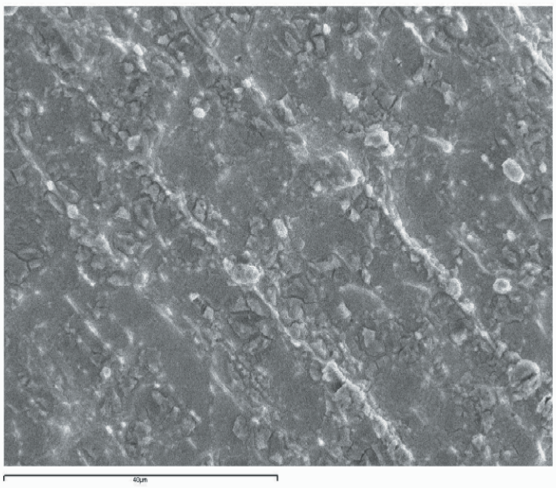

Photo 49

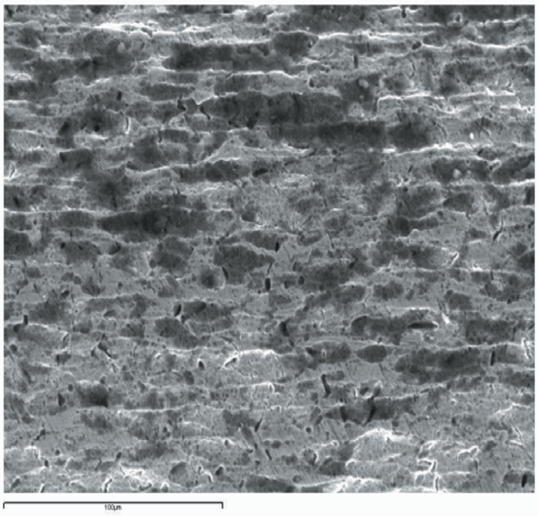

Photo 50

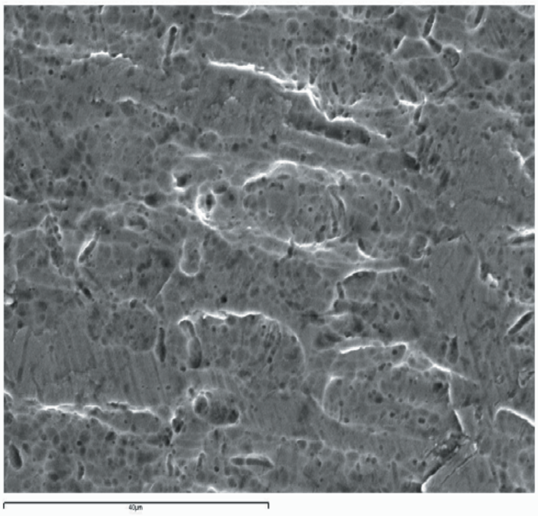

Photo 51

Respond

The as-received state of the wire shows a rough surface topography that resembles an oil painting. Manufacturing lines can be seen at the scan. By-products of the manufacturing process could be responsible of the heterogeneous appearance of the scan at the as-received state (photo 32)

The 30 day immersed wire shows a homogenized surface topography. The wire shows small rosary-like pits as described by Vilar et al[143] at the upper part of the image. This scan is particularly interesting because it shows three different surface topographic corrosive changes. The upper third shows a moderate pitting at a regular surface characterized by the lines present. The medium third still keeps the surface topography typical of the as-received state but less clearly. The lower third shows pitting that differs from the upper third in the sense that elongated corrosion pits can be seen (photo 33)

The polarized scan clearly shows the way that the surface topography of the archwire adopts when affected by polarization. A big cavity can be seen at the wire and also many crater-like structures that indicate loss of metal at the surface that seem to be formed by the adding of pitting. This could be deducted by paying attention to the lower left corner of the scan that seems to be in a less advanced state of corrosion (photo 34)

D-Rect

The as-receive state of the wire seems to be more homogeneous than the Respond. It clearly shows a striated surface topography that keeps a parallelism. The white structures are by-products of the manufacturing of the wire (photo 35)

At the 30 day immersed scan the lining of the surface disappeared. Corrosion pits can be seen that in a particular region. They form an island-like image with an irregular shape. In this scan there are preparation artefacts that were not washed away and that after analyzing them showed to be salts (photo 36)

The polarized specimen shows an image with two different structures. Although incredible, the image shows one of the threads that form the D-Rect archwire that has remained intact after polarization. At the same time, on top of the archwires' surface a corrosion layer can be seen (photo 37)

Stainless Steel 0.016x0.022

The as-received scan shows a regular surface with the finishing lines of the manufacturing procedure that go from the upper part of the image to the lower. The structural topography seems to be quite regular. Some dark spots can be seen and structural defects in white that will be the starting point of corrosion. These surface defects seem to be linked to wire drawing procedures, electropolishing and pickling. The image also shows some characteristic grooves that go from left to the right of the image (photo 38)

The 30 day immersed specimen shows the corrosion that takes place on the wire. It seems to take place at the points that were previously pointed out. Corrosion pits have an elongated shape although small round spots can be also seen. The grooves are now more clearly seen (photo 39)

The image of the polarized specimen shows a big corrosion defect. The crater-like appearance still keeps a trace of the original surface that is a bit darker than the rest and pitting is severe at the lower left side of the image while is not severe at the original and remaining surface (photo 40)

Stainless Steel 0.016

The as-received scan shows a very roughly treated material with clear surface defects that are due to the manufacturing process. Longitudinal scratch lines can be seen in different angular orientations and different kinds of inclusions that result in a variety of geometrical figures (photo 41)

The 30 day immersed scan shows a specimen that seems to be less rough than the scan taken at the as-received state. This does not imply that is less affected by the corrosion. Taking a close look to the scan, more small round pits can be seen in black colour. This view also shows a big surface defect owed to the manufacturing at the lower left corner (photo 42)

The polarized image is very similar to the one obtained for the 0.016x0.022 specimen. It shows a big crater-like defect where two pits can be seen and some of the remaining unaffected surface is still present. Inside the crater some black and white structures can be seen are oxide layers (photo 43)

Nickel Titanium

The as-received scan shows a more homogeneous surface than the so far seem materials. Minor defects can be seen attributable to the manufacturing processes (photo 44)

The 30 day immersed scan does not show big differences when compared to its as-received state. The 30 day immersed scan shows a manufacturing defect and some salts that remained from the electrolyte solution in which it was immersed. But the core of the material keeps the same pattern (photo 45)

The polarized specimen shows the corrosive behaviour of the material which seems to be different to that of the stainless steels. According to the surface analysis of the specimen, the white spots are titanium txide that forms as product of the corrosion. It can also be seen that the material looses it homogeneous aspect and some black clusters form on the surface (photo 46)

Copper Nickel Titanium

The as-received archwire surface seems to be very rough according to the scan shown. It is a very porous material. The pores are homogeneously spread over the surface. No manufacturing defects as drawing lines are seen at the scan (photo 47)

The 30 day immersed specimen shows an increased number of pores and a change in the background surface that now seems to be rougher (photo 48)

At the polarized scan, the surface topography has changed completely. The pores of the material have disappeared and corrosion clusters have formed following a linear orientation (photo 49)

Titanium Molybdenum Alloy

The as-received archwire shows the typically rough surface. It is clear that this surface topography is responsible for the high friction that the wire has (photo 50)

There is no 30 day immersion SEM image due to the fact that this wire did not undergo Ni release testing because it does not contain this element.

The polarized archwire did not show noticeable differences when compared to the as-received specimen. The SEM image was taken at a higher augment but no differences could be seen (photo 51)

3.5 Atomic Force Microscopy

Photos 52 to 87 show the AFM scans obtained for the studied archwires. Three images are shown for each of the as-received and one month immersed specimen. The 3D representation of the depths AFM scan image is shown in the first place to show a general picture of the roughness of the surface.

The 2D depths AFM image (from which the 3D image was obtained) is shown in second place with the RMS areas that were chosen for the statistical analysis. And in the third place, a third image obtained from the deflection data of the probe is shown, it gives a clearer 2D picture of the surface that allows a better qualitative surface comparison among specimens.

They are labelled as follows:

52-54: Respond as-received
55-57: Respond immersed
58-60: D-Rect as-received
61-63: D-Rect immersed
64-66: SS 0.016x0.022 as-received
67-69: SS 0.016x0.022 immersed
70-72: SS 0.016 as-received
73-75: SS 0.016 immersed
76-78: NiTi as-received
79-81: NiTi immersed
82-84: CuNiTi as-received
85-87: CuNiTi immersed

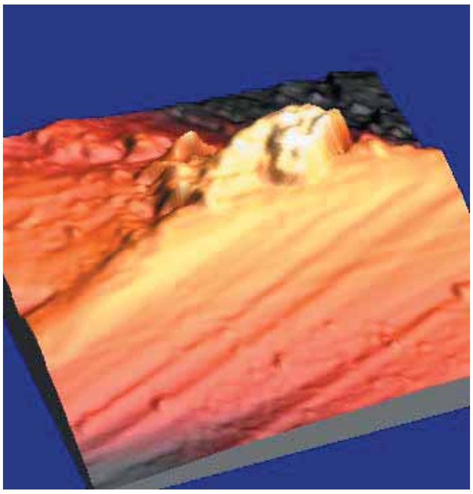

Photo 52

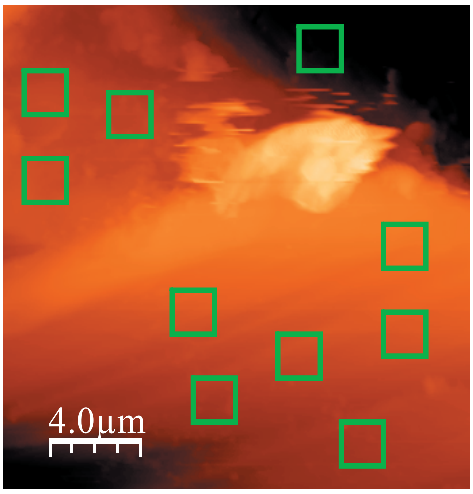

Photo 53

Photo 54

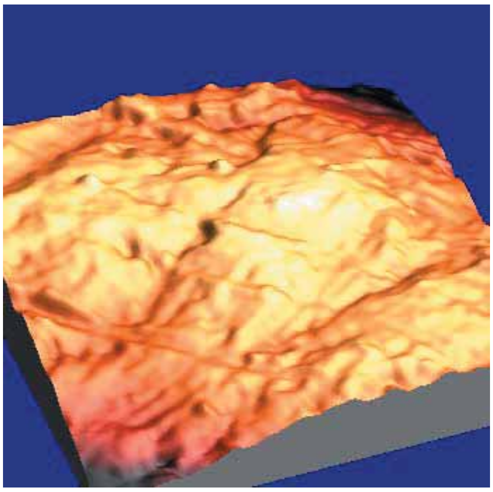

Photo 55

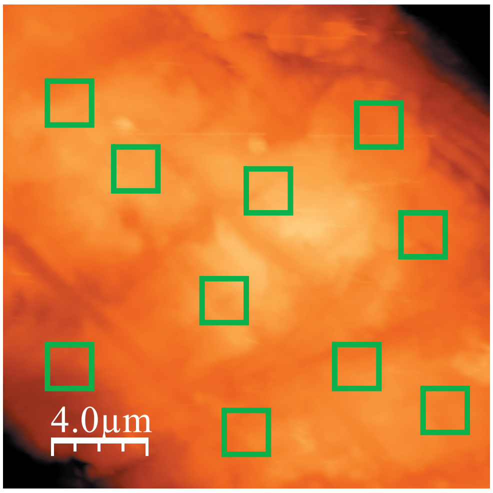

Photo 56

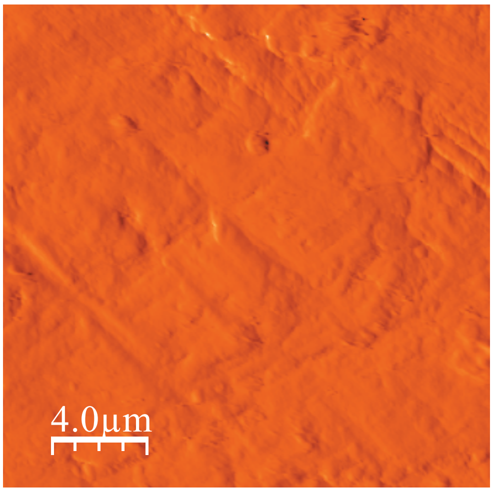

Photo 57

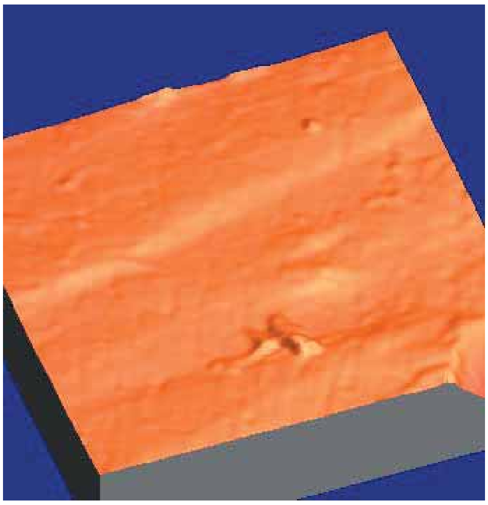

Photo 58

Photo 59

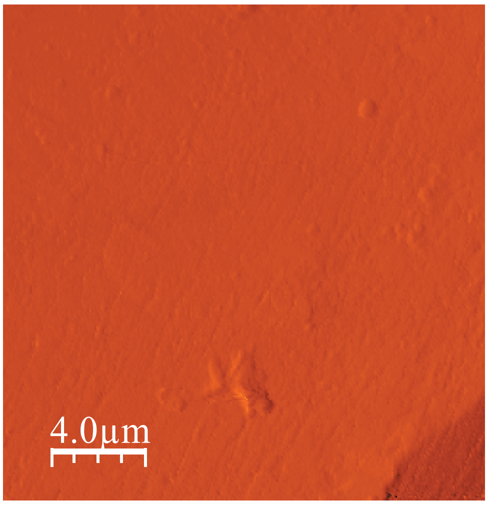

Photo 60

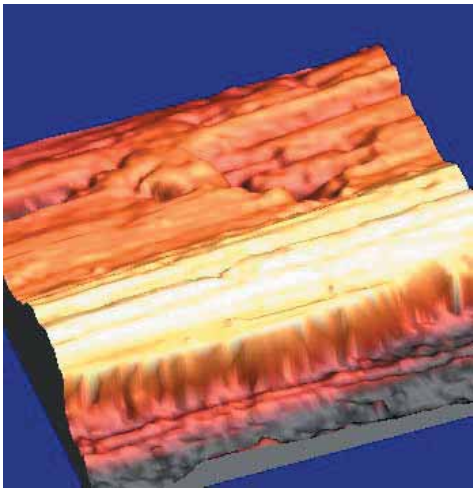

Photo 61

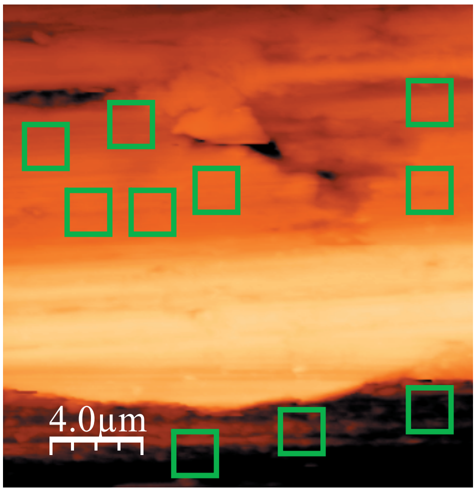

Photo 62

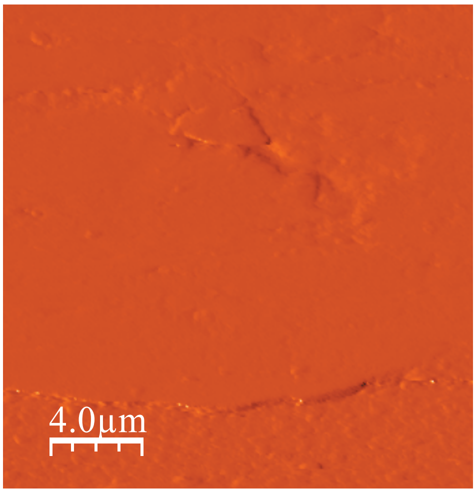

Photo 63

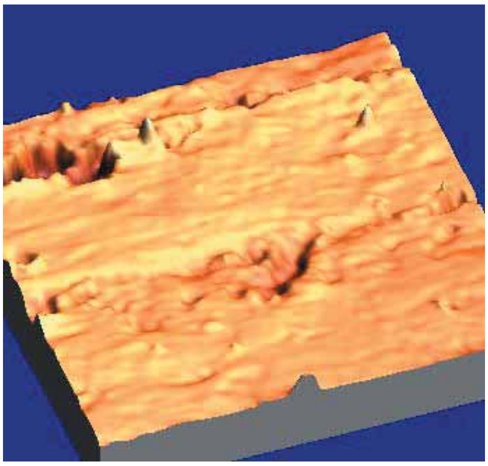

Photo 64

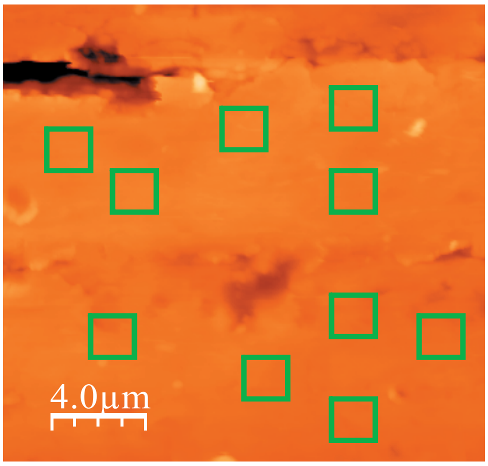

Photo 65

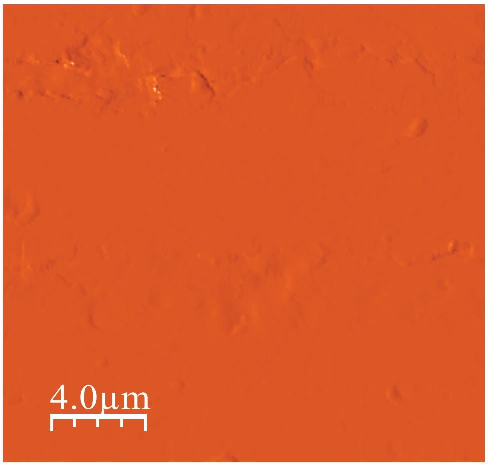

Photo 66

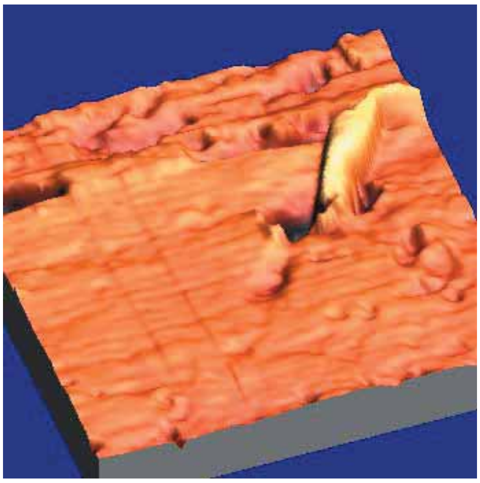

Photo 67

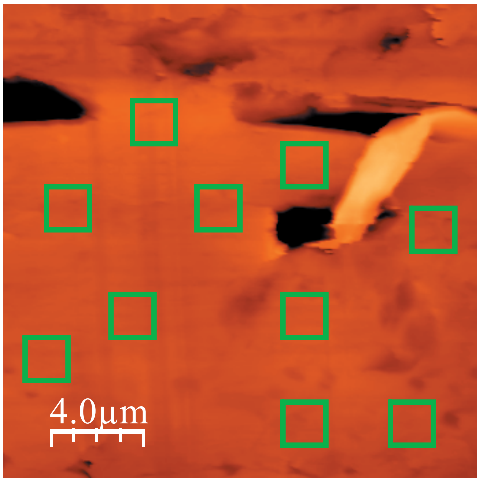

Photo 68

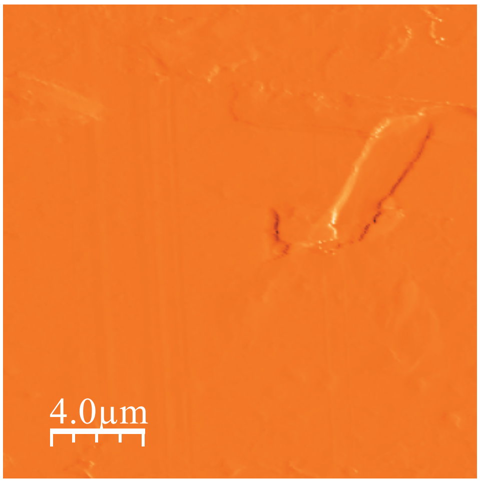

Photo 69

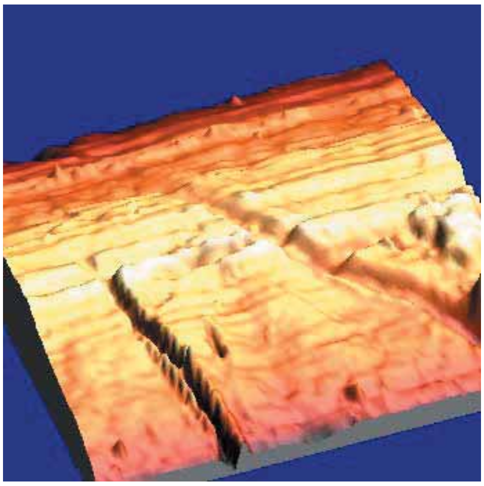

Photo 70

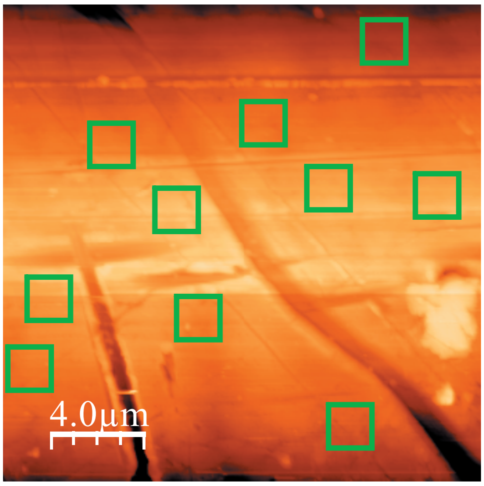

Photo 71

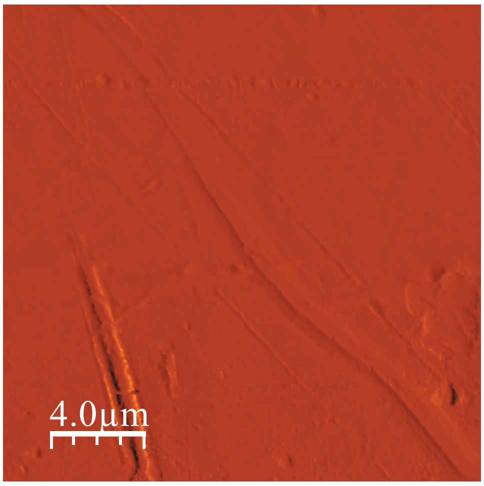

Photo 72

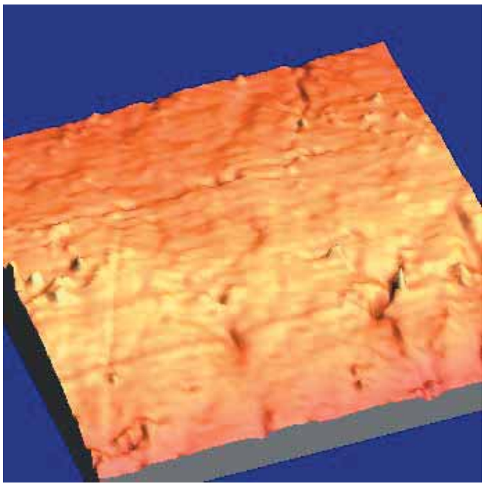

Photo 73

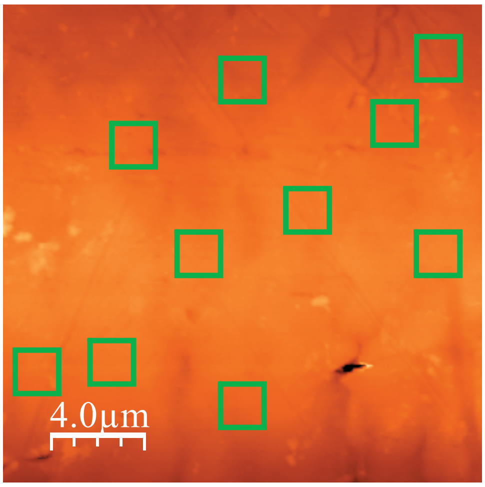

Photo 74

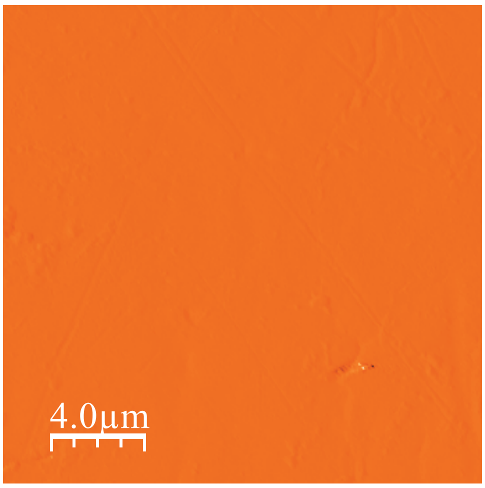

Photo 75

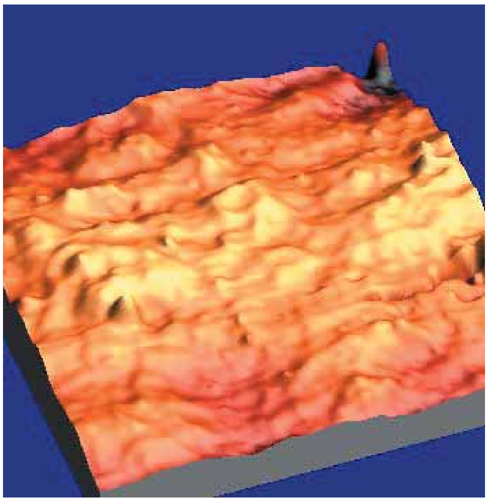

Photo 76

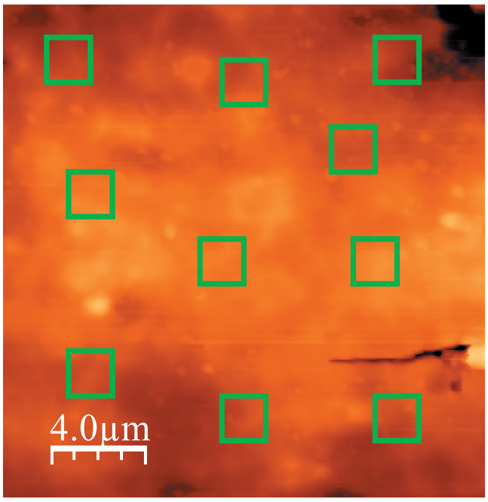

Photo 77

Photo 78

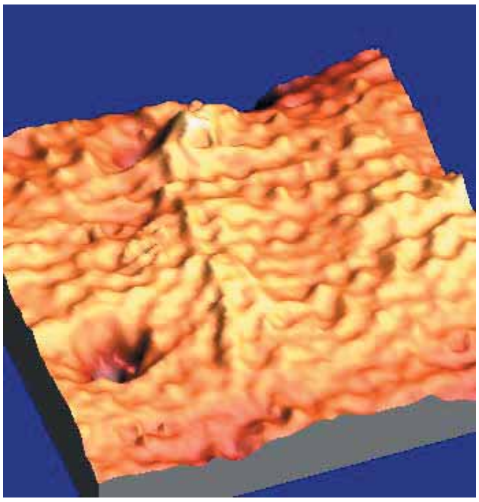

Photo 79

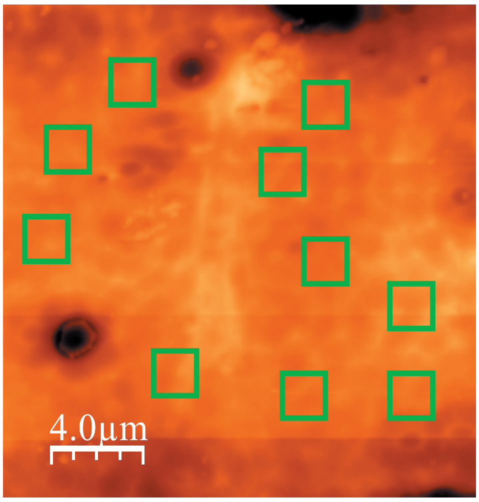

Photo 80

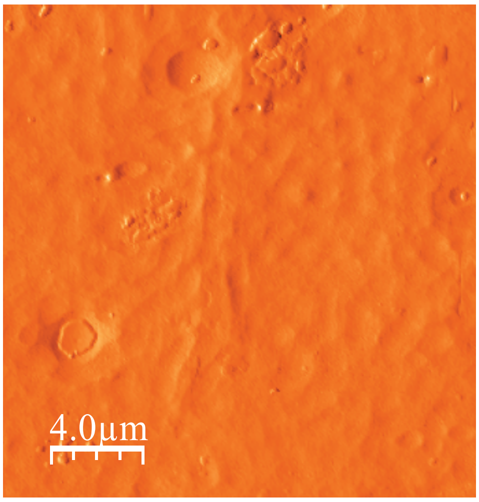

Photo 81

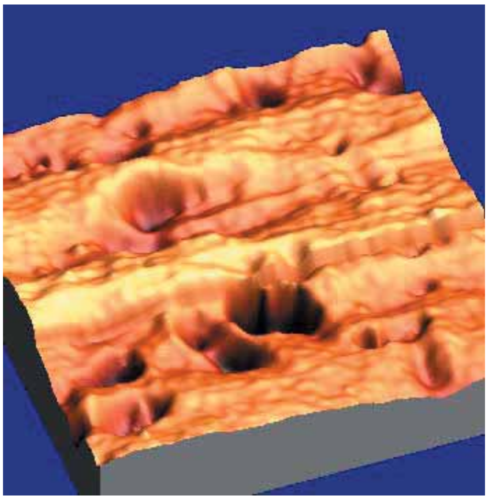

Photo 82

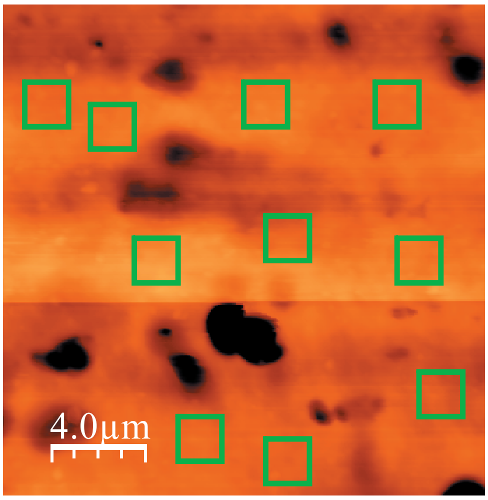

Photo 83

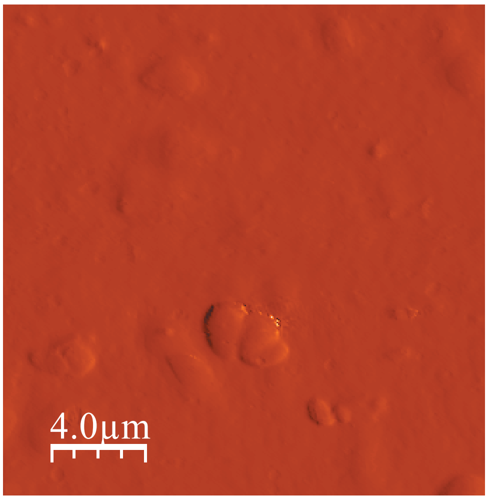

Photo 84

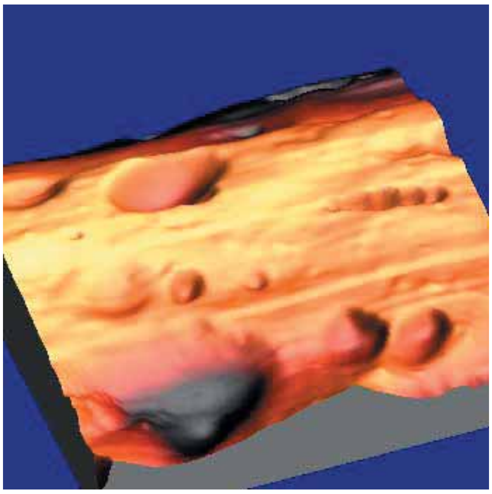

Photo 85

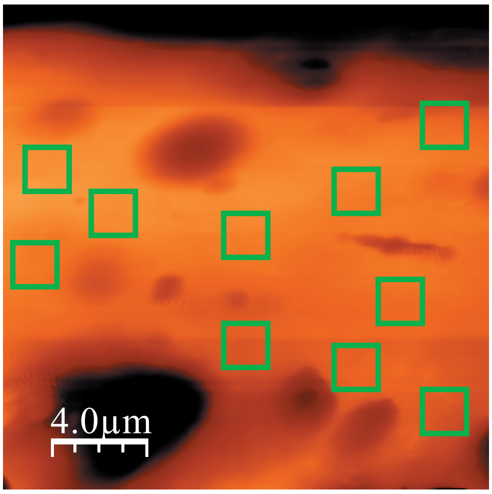

Photo 86

Photo 87

The RMS data gathered from the samples taken from the specimens are shown in tables 5 to 10. Results have been analysed through a t-test in order to obtain the significance of the difference between the RMS value means.

The t_{obs} ratio obtained from the analysis comparing the as-received and immersed state shed the following as gathared at the tables:

Respond: 5,09
D-Rect: 2,70
Stainless Steel 0.016x0.022: 6,67
Stainless Steel 0.016: 3,66
NiTi: 0,55
CuNiTi: 3,63

	As-received			Immersed		
Sample	RMS (micrometers)	Difference to mean	Squared Difference to mean	RMS (micrometers)	Difference to mean	Squared Difference to mean
1	0,012	-0,007563	5,7199E-05	0,02435	-0,003345	1,1189E-05
2	0,02325	0,003687	1,3594E-05	0,0309	0,003205	1,0272E-05
3	0,0214	0,001837	3,37457E-06	0,03612	0,008425	7,09806E-05
4	0,02321	0,003647	1,33006E-05	0,02608	-0,001615	2,60823E-06
5	0,0258	0,006237	3,89002E-05	0,02975	0,002055	4,22302E-06
6	0,01341	-0,006153	3,78594E-05	0,0216	-0,006095	3,7149E-05
7	0,01848	-0,001083	1,17289E-06	0,02038	-0,007315	5,35092E-05
8	0,02396	0,004397	1,93336E-05	0,03173	0,004035	1,62812E-05
9	0,01852	-0,001043	1,08785E-06	0,02656	-0,001135	1,28823E-06
10	0,0156	-0,003963	1,57054E-05	0,02948	0,001785	3,18622E-06

	As-received	Immersed
N	10	10
Mean	0,019563	0,027695
Sum of Squares	0,000201527	0,000210687

Difference of means	0,008132

Estimated source variance	2,29008E-05
Standard deviation	0,001595159

t ratio	5,097924173
degrees of freedom	18

Table 5. Respond

	As-received			Immersed		
Sample	RMS (micrometers)	Difference to mean	Squared Difference to mean	RMS (micrometers)	Difference to mean	Squared Difference to mean
1	0,00869	-0,001875	3,51563E-06	0,01671	-0,007992	6,38721E-05
2	0,00828	-0,002285	5,22123E-06	0,01861	-0,006092	3,71125E-05
3	0,01334	0,002775	7,70063E-06	0,02813	0,003428	1,17512E-05
4	0,0107	0,000135	1,8225E-08	0,03555	0,010848	0,000117679
5	0,0155	0,004935	2,43542E-05	0,08222	0,057518	0,00330832
6	0,01221	0,001645	2,70603E-06	0,01195	-0,012752	0,000162614
7	0,00892	-0,001645	2,70603E-06	0,01325	-0,011452	0,000131148
8	0,0081	-0,002465	6,07623E-06	0,00806	-0,016642	0,000276956
9	0,00731	-0,003255	1,0595E-05	0,02345	-0,001252	1,5675E-06
10	0,0126	0,002035	4,14123E-06	0,00909	-0,015612	0,000243735

	As-received	Immersed
N	10	10
Mean	0,010565	0,024702
Sum of squares	6,70345E-05	0,004354755

Difference of means	0,004287721

Estimated source variance	0,000245655
Standard deviation	0,005224461

t ratio	2,70592483
degrees of freedom	18

Table 6. D-Rect

	As-received			Immersed		
Sample	RMS (micrometers)	Difference to mean	Squared Difference to mean	RMS (micrometers)	Difference to mean	Squared Difference to mean
1	0,00518	2,4E-05	5,76E-10	0,00742	-0,00086	7,396E-07
2	0,00389	-0,001266	1,60276E-06	0,01309	0,00481	2,31361E-05
3	0,00525	9,4E-05	8,836E-09	0,00419	-0,00409	1,67281E-05
4	0,00505	-0,000106	1,1236E-08	0,00696	-0,00132	1,7424E-06
5	0,0063	0,001144	1,30874E-06	0,00474	-0,00354	1,25316E-05
6	0,00698	0,001824	3,32698E-06	0,0056	-0,00268	7,1824E-06
7	0,00475	-0,000406	1,64836E-07	0,01237	0,00409	1,67281E-05
8	0,00475	-0,000406	1,64836E-07	0,0063	-0,00198	3,9204E-06
9	0,00496	-0,000196	3,8416E-08	0,01354	0,00526	2,76676E-05
10	0,00445	-0,000706	4,98436E-07	0,00859	0,00031	9,61E-08

	As-received	Immersed
N	10	10
Mean	0,005156	0,00828
Sum of Squares	7,12564E-06	0,000110472

Difference of means	0,000103347

Estimated source variance	6,53322E-06
Standard deviation	0,000852006

t ratio	3,666641848
degrees of freedom	18

Table 7. SS 0.016

	As-received			Immersed		
Sample	RMS (micrometers)	Difference to mean	Squared Difference to mean	RMS (micrometers)	Difference to mean	Squared Difference to mean
1	0,00479	6,5E-05	4,225E-09	0,00923	-0,0033	0,00001089
2	0,00617	0,001445	2,08803E-06	0,01168	-0,00085	7,225E-07
3	0,00531	0,000585	3,42225E-07	0,01355	0,00102	1,0404E-06
4	0,00375	-0,000975	9,50625E-07	0,02365	0,01112	0,000123654
5	0,00452	-0,000205	4,2025E-08	0,01248	-5E-05	2,5E-09
6	0,00594	0,001215	1,47623E-06	0,00809	-0,00444	1,97136E-05
7	0,00464	-8,5E-05	7,225E-09	0,01709	0,00456	2,07936E-05
8	0,00425	-0,000475	2,25625E-07	0,01071	-0,00182	3,3124E-06
9	0,00375	-0,000975	9,50625E-07	0,01216	-0,00037	1,369E-07
10	0,00413	-0,000595	3,54025E-07	0,00666	-0,00587	3,44569E-05

	As-received	Immersed
N	10	10
Mean	0,004725	0,01253
Sum of Squares	6,44085E-06	0,000214723

Difference of means	0,000208282

Estimated source variance	1,22869E-05
Standard deviation	0,001168422

t ratio	6,679949013
degrees of freedom	18

Table 8. SS 0.016x0.022

	As-received			Immersed		
Sample	RMS (micrometers)	Difference to mean	Squared Difference to mean	RMS (micrometers)	Difference to mean	Squared Difference to mean
1	0,01978	9,6E-05	9,216E-09	0,02109	0,000532	2,83024E-07
2	0,00986	-0,009824	9,6511E-05	0,01712	-0,003438	1,18198E-05
3	0,01889	-0,000794	6,30436E-07	0,01923	-0,001328	1,76358E-06
4	0,01305	-0,006634	4,401E-05	0,01766	-0,002898	8,3984E-06
5	0,02062	0,000936	8,76096E-07	0,02221	0,001652	2,7291E-06
6	0,02567	0,005986	3,58322E-05	0,0225	0,001942	3,77136E-06
7	0,02596	0,006276	3,93882E-05	0,03112	0,010562	0,000111556
8	0,02153	0,001846	3,40772E-06	0,0167	-0,003858	1,48842E-05
9	0,02011	0,000426	1,81476E-07	0,02206	0,001502	2,256E-06
10	0,02137	0,001686	2,8426E-06	0,01589	-0,004668	2,17902E-05

	As-received	Immersed
N	10	10
Mean	0,019684	0,020558
Sum of Squares	0,000223689	0,000179252

Difference of means	-4,44373E-05
Estimated source variance	2,23856E-05
Standard deviation	0,001577113
t ratio	0,554177046
degrees of freedom	18

Table 9. NiTi

	As-received			Immersed		
Sample	RMS (micrometers)	Difference to mean	Squared Difference to mean	RMS (micrometers)	Difference to mean	Squared Difference to mean
1	0,02536	0,004129	1,70486E-05	0,0163	-0,025673	0,000659103
2	0,02101	-0,000221	4,8841E-08	0,05072	0,008747	7,651E-05
3	0,01394	-0,007291	5,31587E-05	0,09161	0,049637	0,002463832
4	0,02806	0,006829	4,66352E-05	0,03871	-0,003263	1,06472E-05
5	0,02066	-0,000571	3,26041E-07	0,01092	-0,031053	0,000964289
6	0,02795	0,006719	4,5145E-05	0,05272	0,010747	0,000115498
7	0,01631	-0,004921	2,42162E-05	0,05507	0,013097	0,000171531
8	0,02492	0,003689	1,36087E-05	0,05057	0,008597	7,39084E-05
9	0,01643	-0,004801	2,30496E-05	0,02923	-0,012743	0,000162384
10	0,01767	-0,003561	1,26807E-05	0,02388	-0,018093	0,000327357

	As-received	Immersed
N	10	10
Mean	0,021231	0,041973
Sum of Squares	0,000235918	0,005025059

Difference of means	0,004789142
Estimated source variance	0,000292276
Standard deviation	0,005698699
t ratio	3,63977837
degrees of freedom	18

Table 10. CuNiTi

3.6 Ni release

A coloured code has been established so to be able to search and compare the information as easily as possible when discussing results.

Green: control group
Red: braided ss wires
Blue: ss wires
Orange: NiTi and CuNiTi wires

From the landmarks at the graph it can be seen which archwire information is being represented because it matches the cross section for that specific wire:

Round red: Respond (0.0175)
Squared red: D-rect (0.016x0.022)
Round blue: ss 0.016
Squared blue: ss 0.016x0.022
Round orange: NiTi (0.016)
Squared orange: CuNiTi (0.017x0.017)

In order to be able to compare results, a calculation regarding the archwires' surfaces exposed to the electrolyte has been done. Therefore archwires Ni leaching is compared for each mm2 exposed. It has to be kept in mind that vials also contained different lengths of wires. Each vial was chosen to contain a full archwire appliance that would have been engaged to an upper arch and a lower arch. In the case of NiTi and CuNiTi, 4 arches by vial were established, 2 upper and 2 lower in each vial. This was done initially because a particular length of arch was thought to be needed in order to perform the test and the as-received braided wires and stainless steels were longer. Anyway, results will be given according to equally exposed surfaces so this is of little concern.

Archwires sizes and calculations on which Ni released test is based are shown in table 11.

	Section (inches)	Section (mm)	Archwire length (mm)	Archwire surface (mm^2)
Respond	0.0175	0,4445	150	209,4628463
D-Rect	0.016x0.022	0,4064x0,5588	150	289,56
SS	0.016	0,4064	150	191,508888
SS	0.016x0.022	0,4064x0,5588	154	297,2816
NiTi (u)	0.016	0,4064	103	131,5027698
NiTi(l)	0.016	0,4064	97	123,8424142
CuNiTi (u)	0.017x0.017	0,4318x0,4318	126	217,6272
CuNiTi (l)	0.017x0.017	0,4318x0,4318	120	207,264

Table 11

Table 12 shows information about analyzed vials.

	Archwires in vial	Total archwire surface (mm^2)
Respond	2	418,92
D-Rect	2	579,12
0.016	2	383
0.016x0.022	2	594,5632
NiTi	2(u)+2(l)	510,68
CuNiTi	2(u)+2(l)	849,76

Table 12

The results obtained from the Ni release test are gathered in table 13.

	Weekly measurements Ni release (ng/mm^2)					
Days	Respond	D-Rect	ss 0,016	ss 0,016x0,022	NiTi	CuNiTi
0	0	0	0	0	0	0
7	0,001368567	0,000876848	0,001758225	0,001248177	0,001218767	0,000871917
14	0,000506541	0,000213773	0,001228721	0,000987481	0,000379024	0,000783892
30	0,000290843	0,000212046	0,000633629	0,00043299	0,000438631	7,63039E-05

Table 13

The resulting graph according to the above table is labelled is graph 25.

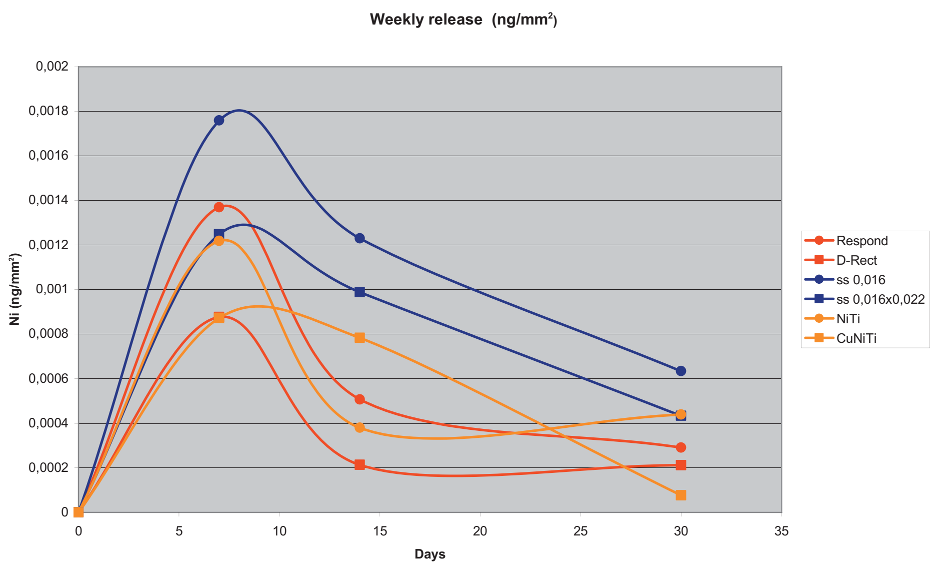

Graph 25

Table 14 shows values of Ni released if accumulated quantities of released Ni according to the particular archwires embedded surfaces are taken into account.

	Accumulated Ni release values (ng/mm²)					
Days	Respond	D-Rect	ss 0,016	ss 0,016 x 0,022	NiTi	CuNiTi
0	0	0	0	0	0	0
7	0,00136857	0,000876848	0,00175822	0,001248177	0,00121877	0,00087192
14	0,00187511	0,00109062	0,00298695	0,002235658	0,00159779	0,00165581
30	0,00216595	0,001302666	0,00362057	0,002668648	0,00203642	0,001

Table 14

The graph obtained from the above accumulated values is graph 26.

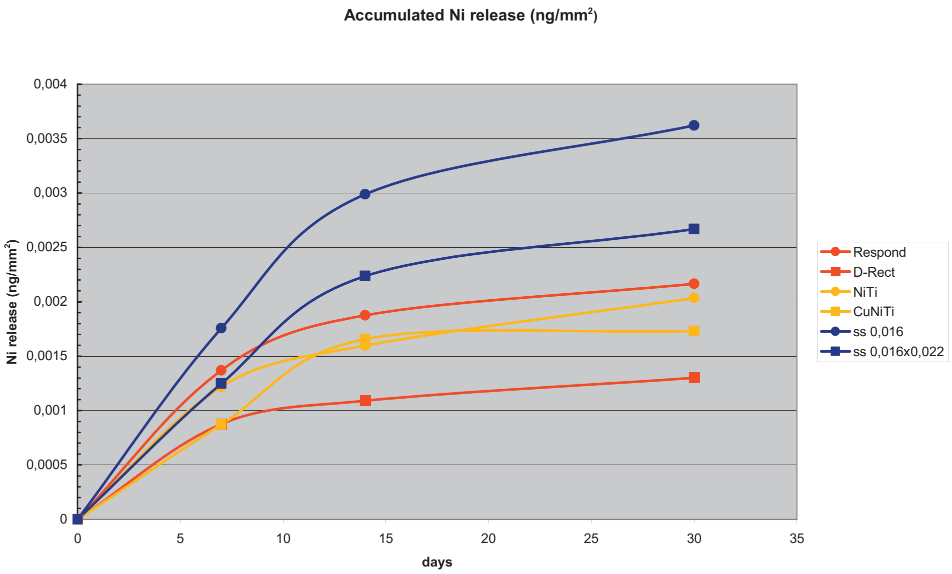

Graph 26

3.7 Differential Scanning Calorimetry

Results obtained are shown in graphs 27 to 40. Tables 15 and 16 depict the numerical results obtained from the graphs for the phase transition temperatures.

The difference among the gathered data on tables 15 and 16 relies on the criteria followed when establishing the phase transition temperature starting point. Some studies establish the point as the value were a deviation from the baseline value starts (table 15) and others take it as the intersection of the tangent to the slope of the heat flow curve to the corresponding hypothetical baseline value (table 16). Both of them have been shown for discussion purposes. This leads to graphs 27 to 40. These graphs have been presented showing the as-received DSC, the 30 day immersed DSC test and finally the polarized sample DSC. First, DSC graphs according to criteria followed in table 16 are shown and later the same graphs are transformed for the phase transition temperatures used in table 15.

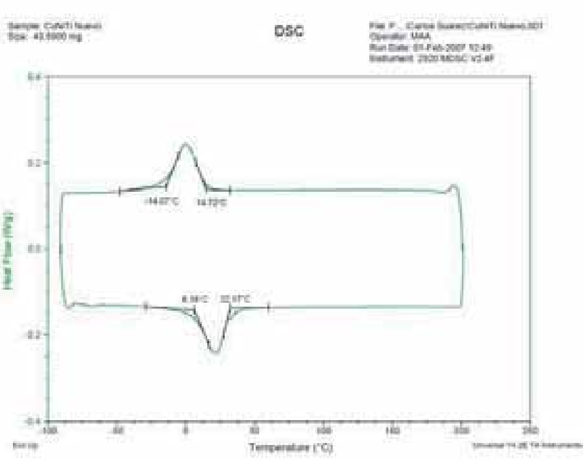

Graph 27

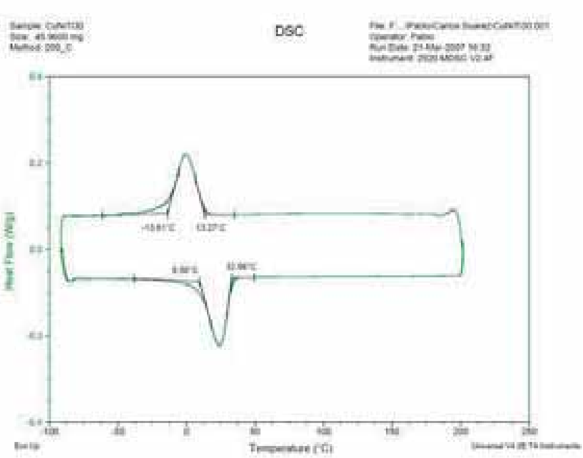

Graph 28

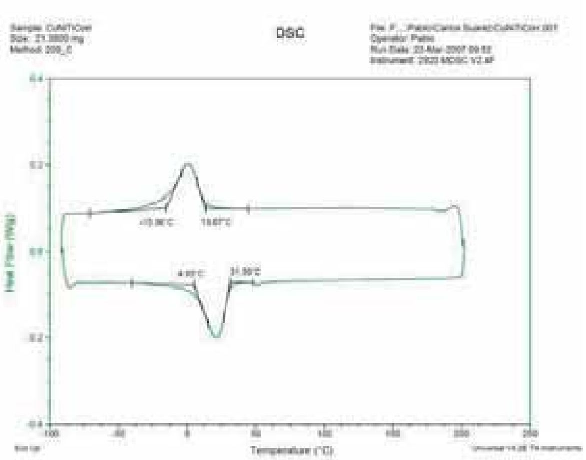

Graph 29

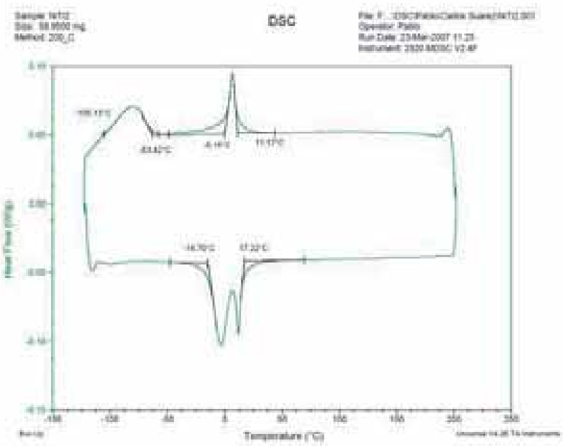

Graph 30

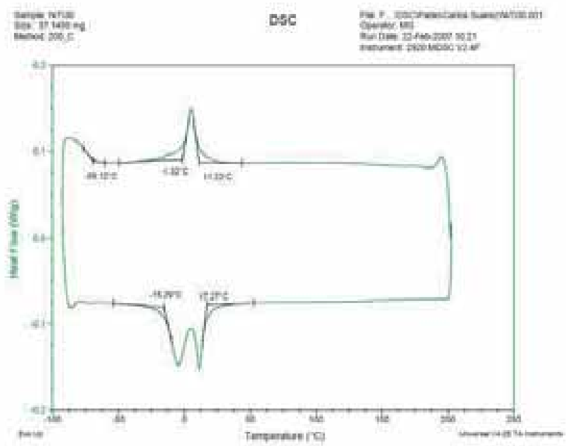

Graph 31

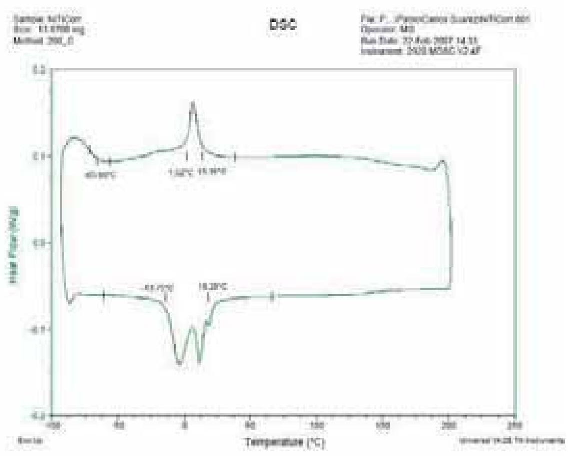

Graph 32

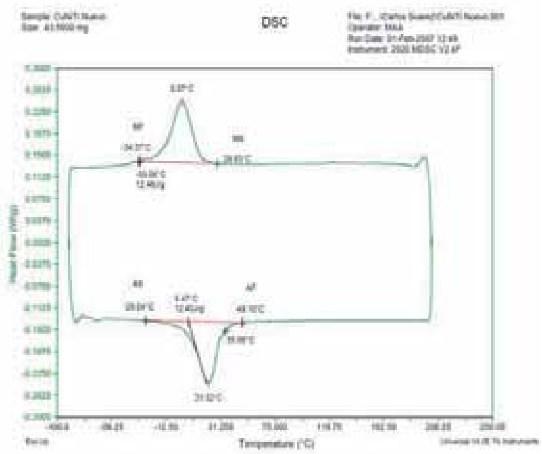

Graph 33

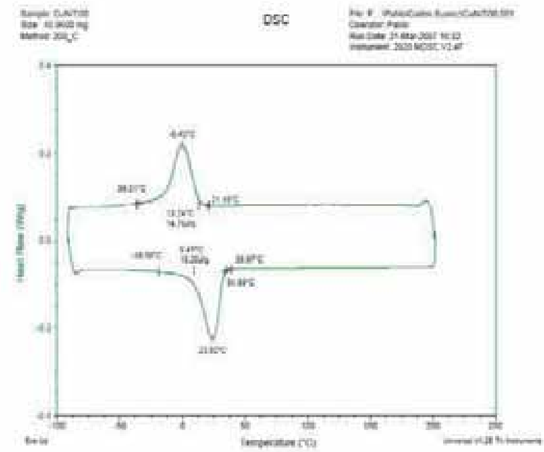

Graph 34

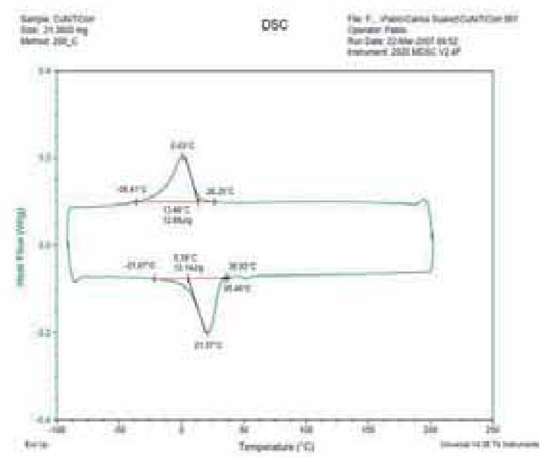

Graph 35

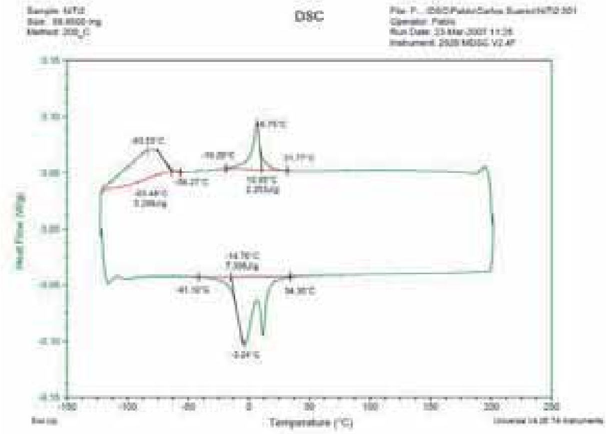

Graph 36

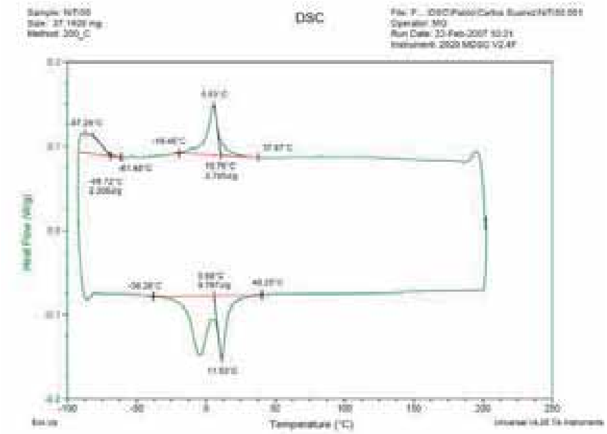

Graph 37

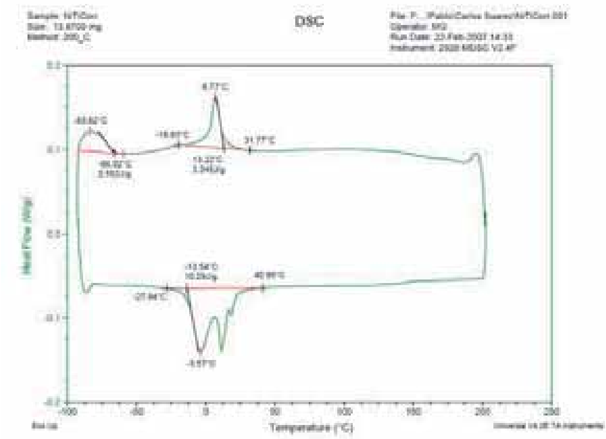

Graph 38

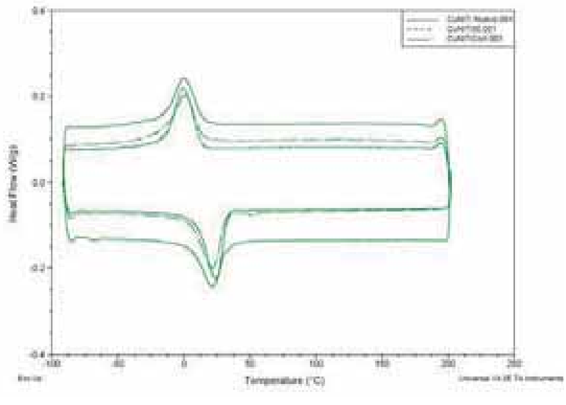

Graph 39

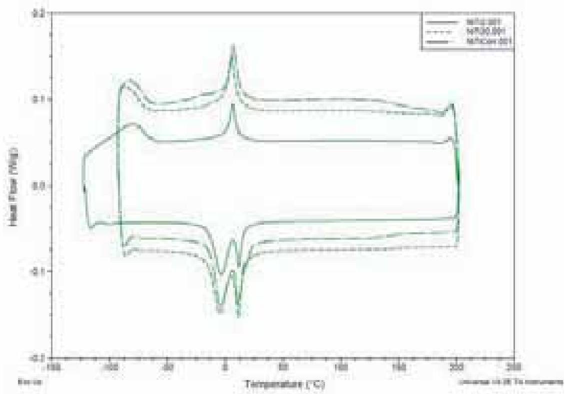

Graph 40

	NiTi			CuNiTi		
	as-received	30 day immersed	polarized	as-received	30 day immersed	polarized
As	-41,1	-38,26	-27,94	-29,04	-18,56	-21,67
Af	34,3	40,25	40,99	49,1	38,97	36,93
Rs (M)	31,77	37,67	31,77			
Rf (M)	-19,2	-19,46	-19,83			
Ms	-56,27	-61,48	-66,02	28,83	21,15	26,25
Mf				-34,57	-36,01	-36,41

Table 15

	NiTi			CuNiTi		
	as-received	30 day immersed	polarized	as-received	30 day immersed	polarized
As	-14,7	-15,29	-13,75	6,18	9,5	4,95
Af	17,22	17,27	18,2	32,17	32,96	31,5
Rs (M)	11,17	11,23	13,36			
Rf (M)	-0,16	-1,32	1,52			
Ms	-63,42	-69,12	-65,68	14,72	13,27	13,67
Mf	-105,13	?	?	-14,07	-13,81	-15,56

Table 16